

**Characterization of Photocatalyst for Degradation of
Diisopropanolamine (DIPA) Using Photo-Fenton**

by

Adnin Itriah Binti Rosli

Dissertation submitted in partial fulfillment of
the requirements for the
Bachelor of Engineering (Hons)
(Chemical Engineering)

SEPTEMBER 2012

Universiti Teknologi PETRONAS
Bandar Seri Iskandar
31750 Tronoh
Perak Darul Ridzuan

CERTIFICATION OF APPROVAL

**Characterization of Photocatalyst for Degradation of
Diisopropanolamine (DIPA) Using Photo-Fenton**

by

Adnin Itriah Binti Rosli

A project dissertation submitted to the
Chemical Engineering Programme
Universiti Teknologi PETRONAS
in partial fulfillment of the requirement for the
BACHELOR OF ENGINEERING (Hons)
(CHEMICAL ENGINEERING)

Approved by,

(Putri Nadzrul Faizura Megat Khamaruddin)

UNIVERSITI TEKNOLOGI PETRONAS
TRONOH, PERAK

January 2012

CERTIFICATION OF ORIGINALITY

This is to certify that I am responsible for the work submitted in this project, that the original work is my own except as specified in the references and acknowledgements, and that the original work contained herein have not been undertaken or done by unspecified sources or persons.

ADNIN ITRIAH BINTI ROSLI

ABSTRACT

Alkanolamines such as diisopropanolamine (DIPA) are used to treat natural gas in order to remove the acid gases, such as carbon dioxide, CO₂ and hydrogen sulfide, H₂S in it. The wastewater of this process contained high amount of the amines in which causes the COD reading to be high. Therefore, methods of degrading the recalcitrant pollutant were introduced using photo-Fenton reaction, in which Fe catalysts is added into the wastewater and the reaction took place under the illumination of light. The wastewater undergo oxidation process producing •OH radical which later will react with the amines and degrade them. Focusing on one method to synthesize the catalysts, few catalysts were developed to help in the degradation process of DIPA. The catalysts are characterized and tested in the wastewater in the presence of UV and visible light. The catalysts are characterized in order to obtain the suitable catalysts that will give higher DIPA degradation in the wastewater.

ACKNOWLEDGEMENT

My utmost gratitude goes to the Almighty God whom without His help by giving good health and time, I am unable to finish my project successfully.

This project would not be completed successfully without the assistance and guidance from individuals. Therefore, I owe my deepest gratitude to my supervisor, Madam Putri Nadzrul Faizura Megat Khamaruddin for her useful guidance, complete trust, and strong encouragement given. Thank you for the knowledge accommodated and the continuous support throughout the project.

Sincerest gratitude goes to Miss Raihan Mahirah Ramli for her valuable input and guidance in laboratory training. To the Final Year Research Paper and Project Coordinators, Dr Anis Suhaila bt Shuib (FYP I) and Dr Norhayati Mellon (FYP II), thank you for coordinating the series of trainings and talks, useful information, and quick respond towards the project completion. I thank all staffs of Chemical Engineering Department intentionally and unintentionally for any guidance and information regarding this course.

Last but not least, my warmest thanks to my dear family and friends who always give me undivided support and wonderful motivations I most certainly need to keep me driven.

TABLE OF CONTENTS

CHAPTER 1:	INTRODUCTION.....	1
	1.1 Background of Study.....	1
	1.2 Problem Statement.....	3
	1.3 Objectives.....	4
	1.4 Scope of Studies.....	4
CHAPTER 2:	LITERATURE REVIEW.....	5
CHAPTER 3:	METHODOLOGY.....	9
	3.1 Chemicals.....	9
	3.2 Experimental Procedure.....	10
CHAPTER 4:	RESULT AND DISCUSSION.....	14
	4.1 Catalyst Characterization.....	19
	4.2 Catalyst Performance Study.....	20
CHAPTER 5:	CONCLUSIONS AND RECOMMENDATIONS.....	21
	5.1 Conclusion.....	27
	5.2 Recommendation.....	28
REFERENCES.....		29
APPENDICES.....		32

LIST OF FIGURES

Figure 3.1: Summary of wet impregnation catalyst preparation method.....	10
Figure 3.2: Flowchart of experimental procedure.....	13
Figure 4.1: The degrading temperature of 0.3 wt% Fe catalyst.....	14
Figure 4.2: The degrading temperature of 0.7 wt% Fe catalyst.....	15
Figure 4.3: The degrading time of 0.3 wt% Fe catalyst.....	16
Figure 4.4: The degrading time of 0.7 wt% Fe catalyst.....	16
Figure 4.5: Image of 0.3 wt% Fe catalyst calcine at 600°C for 2h.....	17
Figure 4.6: Image of 0.7 wt% Fe catalyst calcine at 600°C for 2h.....	18
Figure 4.7: Energy dispersive X-ray spectrometry (EDX) of 0.3 wt% Fe, 600°C, 2h...	18
Figure 4.8: Energy dispersive X-ray spectrometry (EDX) of 0.7 wt% Fe, 600C, 2h....	19
Figure 4.9: The range of wavelength for catalyst calcine at 600°C.....	21
Figure 4.10: DIPA degradation rate for 0.3 and 0.7wt% of Fe catalysts calcined at 600°C for 1h and 2h under UV illumination.....	22
Figure 4.11: DIPA degradation rate for 0.3 and 0.7 wt% of Fe catalyst calcined at 700°C for 1h and 2h under UV illumination.....	23
Figure 4.12: DIPA degradation rate for 0.3 and 0.7 wt% of Fe catalyst calcined at 600°C for 1h and 2h under visible illumination.....	24
Figure 4.13: DIPA degradation rate for 0.3 and 0.7 wt% of Fe catalyst calcined at 700°C for 1h and 2h under visible illumination.....	25

LIST OF TABLES

Table 1.1: Redox potential standards of some oxidant species.....	2
Table 3.1: List of chemicals used in this project.....	9
Table 3.2: List of equipments used in this project.....	11
Table 3.3: The standards of HPLC.....	12
Table 4.1: BET surface area of the catalysts.....	19
Table 4.2: Average pore width of the catalysts.....	20

CHAPTER 1

INTRODUCTION

1.1 BACKGROUND OF STUDY

1.1.1 Wastewater contaminated with DIPA

Amine solutions are used to remove hydrogen sulfide (H_2S) in the gas sweetening process. There are two principle amine solutions used, monoethanolamine (MEA) and diethanolamine (DEA). Being the secondary amine of the alkanolamine group, diisopropanolamine (DIPA) is used to remove hydrogen sulfide (H_2S) and carbon dioxide (CO_2) from gasses. DIPA systems are similar to MEA systems but it offer more advantages such as the carbonyl sulfide (COS) can be removed and regenerated easily and the system is generally noncorrosive and requires less heat input. Wastewater contaminated with DIPA is constantly generated.

Water that has been polluted by this organic pollutant cannot be easily discharged into the mainstream. Plus, high Chemical Oxygen Demand (COD) of the contaminated wastewater make it impossible to be treated by the conventional wastewater treatment. Since the wastewater that has been highly contaminated with DIPA is sent to the contractor to be disposed, the disposal cost will be relatively high due to large volume of wastewater generated. Pretreatment of waste is necessary before entering the wastewater treatment plant to meet the standard of requirement.

1.1.2 Technology to treat wastewater contaminated with DIPA

Treatment technology to degrade this organic compound is still need to be developed. Advanced Oxidation Processes (AOPs) have proved their abilities to mineralize organic contaminants present in wastewater. The main feature of AOPs is hydroxyl radical (OH°) which has a high oxidation potential and acts rapidly with most organic

compounds. Table 1.1 below shows the redox potential standards of some oxidant species. Hydroxyl radicals possess the redox potential value of 2.80V which is higher compared to other oxidants. Fluorine possesses the highest redox potential value which is 3.03V. However, fluorine is not suitable to be used in the experiment due to environmental issues.

Table 1.1: Redox potential standards of some oxidant species

Oxidant	Redox Potential, E°, V.
Fluorine	3.03
Hydroxyl radical	2.80
Atomic oxygen	2.42
Ozone	2.07
Hydrogen peroxide	1.77
Permanganate ion	1.67
Chlorine	1.36
Chlorine dioxide	1.27

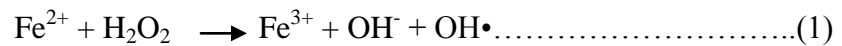
Among the AOPs, Fenton's oxidation is the simplest process which involves only ferrous catalyst and hydrogen peroxide. The degradability of DIPA was measured by the reduction of DIPA concentration in the treated wastewater sample. High percentage of DIPA degradation is observed using the Fenton's oxidation process. However, biological treatment is still needed in order to complete the degradation process. Various methods are carried out to increase the degradability efficiency of the process. One of the ways to further increase the COD removal of organic compounds in wastewater is using photo-Fenton process. Photo-Fenton, which is the reaction of Fenton's reagent with hydrogen peroxide (H_2O_2) aided by the light source is invented by the researcher. Using this process, higher COD removal can be obtained compared to the Fenton's oxidation process.

1.1.3 Catalyst

Catalyst is needed in the photodegradation study. To obtain a high percentage of DIPA degradation, catalyst that is going to be used must have a high durability and resistance to prevent itself from degrading together with DIPA. In modified photo-Fenton process, Fe/TiO₂ catalyst is used instead of Fe catalyst only. The catalysts will be synthesized using wet impregnation method. Characterization of catalyst involves the process of determining the properties of the catalyst using several equipments. Performance study will be conducted to test the synthesized catalysts in the wastewater containing DIPA. This study is important to determine the best catalyst with higher percentage of DIPA degradation.

1.2 PROBLEM STATEMENT

Fenton oxidation has proved its capability of degrading the wastewater contaminated with DIPA. However, this system still required extended duration for complete removal of organic compounds. Since the degradation efficiency for the oxidation process can be accelerated by irradiation with UV light, photo-Fenton system is used instead of Fenton system. Using this system, complete mineralization is achieved in shorter time compared to the previous system.



In photo-Fenton process, homogeneous catalyst which is the ferrous ion (Fe²⁺) is used in the presence of hydrogen peroxide (H₂O₂). The reaction between Fe and H₂O₂ will produce (OH°) which is essential in the degradation process. Fe³⁺ ion which is the by-product of the reaction will dissolve into the solution. A fine ferric sludge will form when the solution pH was increased during the neutralization stage. The formation of sludge will be a drawback of this process as this will requires a sludge handling system prior to disposal of treated water. Plus, it is difficult to retrieve the ferrous ion Fe²⁺ used during the reaction.

When the heterogenous catalyst is used instead of homogeneous catalyst, the catalyst separation process is expected to be easier. The resultant effluent from the system also

will be free from any sludge or suspended solid originating from Fenton's reagent. Modified photo-Fenton system used the concept of heterogeneous catalyst. The catalyst is modified into powder form where the TiO_2 catalyst is introduced to be the support to the Fe catalyst. This Fe/ TiO_2 catalyst is used in the photo-Fenton process in the presence of light in order to increase the percentage of DIPA degradation.

Various method can be use to dope the Fe catalyst to the TiO_2 catalyst. The most common method that usually used is wet impregnation method. The catalysts are characterized and tested using the wastewater in the presence of UV and visible light in order to obtain the suitable catalysts that will give higher rate of DIPA degradation in the wastewater.

1.3 OBJECTIVES

- 1) To synthesize catalyst for photocatalytic oxidation of DIPA.
- 2) To characterize the catalyst that has been prepared.
- 3) To study the performance of synthesized catalyst using visible and UV light.

1.4 SCOPE OF STUDIES

This work has been undertaken to experimentally synthesize the catalyst for further usage in degradability of diisopropanolamine (DIPA) using modified photo-Fenton's process. One method will be used to dope the Fe to TiO_2 to form Fe/ TiO_2 catalyst which is wet impregnation method. The catalyst will be synthesized by varying the weight percent (wt%) of Fe in ferric solution, calcinations temperature and time. After that, the catalyst needed to be characterized to know its physical properties. The crystal structure, morphology, light adsorption, and photocatalytic properties of the catalysts were examined by X-ray Diffraction, Field Emission Electron Microscopy, and Ultraviolet-Visible Spectrophotometry. The performance of the synthesized catalyst under visible and UV light will be observed.

CHAPTER 2

LITERATURE REVIEW

2.1 Usage of amine group in gas sweetening process

Natural gas from some wells contains significant amounts of carbon dioxide and sulfur. This natural gas, is commonly called 'sour gas' due to the rotten smell provided by its sulfur content. Sulfur exists in natural gas as hydrogen sulfide (H_2S). If the hydrogen sulfide content exceeds 5.7 milligrams of H_2S per cubic meter of natural gas, the gas is considered as sour (Processing Natural Gas, retrieved: June 2012). 'Sweetening' the gas is referred to the process of removing hydrogen sulfide (H_2S) and carbon dioxide (CO_2) from natural gas. This treating unit is commonly used in refineries, petrochemical plants, natural gas processing plants and also some other industries. Amine solutions are used in an absorption process to remove the hydrogen sulfide (H_2S) from the produced gas.

Triethanolamine (TEA) was the first alkanolamine to be used in the early gas treating plants. The potential of alkanolamine as absorbent for acidic gases was discovered in 1930 by R. R. Bottoms. Since then, other members of alkanolamines such as monoethanolamine (MEA), diethanolamine (DEA), diisopropanolamine (DIPA), methyldiethanolamine (MDEA) were introduced in the market and evaluated as possible acid gas absorbents (Kohl et al, 1997). Water pollution caused by these organic pollutants will likely increase proportional to the alkanolamines usage. Development of technology is needed to degrade these organic compounds in wastewater effluent since they are used widely these days.

2.2 Wastewater treatment technology

Advance Oxidation Process (AOPs) showed a great potential to become the most favorable process in wastewater treatment. Hydroxyl radical (OH°) which is the main feature of AOPs, has a high oxidation potential and acts rapidly with most organic

compounds. Several methods can be found to produce hydroxyl radical (OH°), however, AOPs has the potential to degrade wide range of organic compounds which is impossible to be degraded by other methods. Using hydrogen peroxide photolysis, AOPs has been proven to degrade organic compounds such as dyes, aromatic hydrocarbons, amines, pharmaceutical molecules and mineral oils at low initial pH values (2-5) (Lou et al (1995) & Gulkaya et al (2006)). Nitrophenols, using Fenton and photo-Fenton reagent has also been degraded in a study (Goi et al, 2002).

Fenton and photo-Fenton oxidation process are examples of AOPs. Involving only ferrous catalyst and hydrogen peroxide (H_2O_2), highly reactive hydroxyl radical (OH°) will be produced with the potential of 2.8V. This was first reported in 1876 by Fenton (Matthew, 2003). Using Fenton's reagent, biodegradation of monoethanolamine (MEA) and diethanolamine (DEA) achieved complete degradation in 24 hours (Sabantti et al, 2009, Dutta et al, 2010). Removal of organic compounds occurs slowly, therefore, extended duration is needed for it to complete.

2.3 Advantages of heterogeneous catalyst

At optimum condition, (pH=3, molar ratio of 10 for $\text{H}_2\text{O}_2 : \text{Fe}^{2+}$) COD removal of 73% was reported for degradation of waste water contaminated with diisopropanolamine (DIPA) (Omar et al, 2010). Major disadvantage of this process is the formation of the sludge from Fe^{3+} ion. Since Fe^{3+} ion dissolved into the solution, it is difficult to retrieve the ferrous ion, Fe^{2+} ion back (Vinita et al, 2010). Thus, replacement of homogeneous catalyst with a heterogeneous catalyst is hoped to prevent this problem from happening.

Homogeneous catalyst occurs when the catalyst operates respectively in the same phase with the reactant such as Fe^{2+} which react in liquid phase to form Fe^{3+} ion, hydroxyl radical (OH°), and hydroxide ion (OH^-) in liquid state. Heterogeneous catalyst involves the reaction of catalyst in different phases from the reaction. Example of heterogeneous catalysis involved is between powder catalysts in form solid with the presence of liquid hydrogen peroxide (H_2O_2) where the reaction occurs in liquid form.

Some of the photo-Fenton reaction utilizes the concept of heterogeneous catalysis. The photocatalytic efficiency increases to 76% (highest of all samples) using F-Fe codoped

TiO₂ where heterogeneous catalysis is applied (Zhang et al, 2011). Application of photocatalytic oxidation utilizing Fe/TiO₂ under UV radiation was reported widely to degrade broad range of recalcitrant organic compounds such as phenol (Adan et al, 2009), dyes (Asilturk et al, 2009), and pesticides (Banic et al, 2011) with superior photocatalytic activity compared to bare TiO₂. Apart of that, photocatalytic oxidation utilizing TiO₂ – and Pt/TiO₂ – assisted photocatalyst under UV radiation was also reported widely to degrade broad range of recalcitrant organic compounds such as ethylamine, diethylamine, ethanolamine, diethanolamine and triethanolamine. This is proven when 55-80% of the total nitrogen recovered from initial nitrogen concentration was collected after the experiment (Klare et al, 2000). Another alkanolamine, 2-dimethylamino-2-methyl-1-propanol (DMAMP), was also studied in the photocatalytic oxidation system utilizing TiO₂ (Lu et al, 2009).

The rate of degradation of organic pollutant with Fenton reagents can strongly accelerated by irradiation with UV-light. The combination of UV light with Fenton (photo-Fenton) is advantageous, not only it leads to ferrous catalyst recycling by reduction of Fe³⁺. By this, the concentration of Fe²⁺ increases and therefore the reaction is accelerated. The increased in efficiency of the photo-Fenton process is attributed to the photo reduction of ferric ion, the efficient use of light quanta and the photolysis of Fe³⁺ organic intermediate chelates.

2.4 Reasons of choosing TiO₂ and DIPA in the experiment

TiO₂ make a suitable candidate for the as the catalyst support due to the small ionic radius of Fe³⁺ (0.645 Å) which is compatible to ionic radius of Ti⁴⁺ (0.605 Å) (Khan et al, 2008). DIPA is chosen as the organic pollutant in this experiment because it is reported that COD value of DIPA is very high which is 17 000ppm (Omar et al, 2010) while the value given by the local authority is only 100 ppm (Environmental quality (sewage and industrial effluents) regulation, 1979).

2.5 Methods available to prepare the catalyst

The catalyst was synthesized before it is use in the photodegradation process. There are many methods of synthesise including wet impregnation and co-precipitation. Wet Impregnation method will be used in synthesizing the catalyst in this experiment. These two main reactions were used widely to prepare catalyst which has been used in photodegradation process involving recalcitrant organic compounds such as ethylamine, diethylamine, ethanolamine, diethanolamine and triethanolamine (Klare et al, 2000).

2.6 Conclusion

Until now, no study was reported on the application of Fe/TiO₂ for the degradation of DIPA. Therefore, this study is carried out to test the effectiveness of modified photo-Fenton to degrade this organic pollutant which is widely utilized in natural gas processing plant. Catalyst will be synthesized based on the Wet Impregnation method. The catalyst that has been prepared will be characterized. Lastly, the performance of the catalyst will be studied under the reaction of visible and UV light.

CHAPTER 3

METHODOLOGY

This chapter explains on the experimental part of the project work, including description on the chemicals, procedure and operation of the experiment and analytical methods. The details of each experiment are also elaborated in this chapter. Basically, the experiment is divided in three main activities. Those activities are catalyst synthesizing, characterization of catalyst as well as catalyst performance study.

3.1 CHEMICALS

Table 3.1 below shows the list of chemicals used in this project.

Table 3.1: List of chemicals used in this project

Chemicals	MW (g.mol⁻¹)	T_m (°C)	T_b (°C)	ρ (T = 25°C) (kg.m⁻³)
DIPA	133.19	44	249	0.989
Hydrogen Peroxide (H ₂ O ₂)	34.00	-	-	1.11
Iron (III) nitrate nonahydrate (Fe(NO ₃) ₃ .9H ₂ O)	404.00	47	-	1168000
TiO ₂ P25	79.87	1850	-	4260
Glycerol	92.00	17.8	290	1261000

3.2 EXPERIMENTAL PROCEDURE

3.2.1 Catalyst Preparation

Supported titanium dioxide catalysts are widely used in a number of industrial processes. The role of the support may be to improve the properties such as stability of the active components or to participate directly in the catalytic reaction, for example, by providing acidic sites. The activity of the supported catalysts is strongly dependent on the preparation method used and on the choice of reagents and support. One method used to prepare Fe/TiO₂ catalyst in this project is wet impregnation method. Figure 3.1 below shows the summary of the procedures to prepare the Fe/TiO₂ catalyst.

3.2.1.1 Wet Impregnation Method

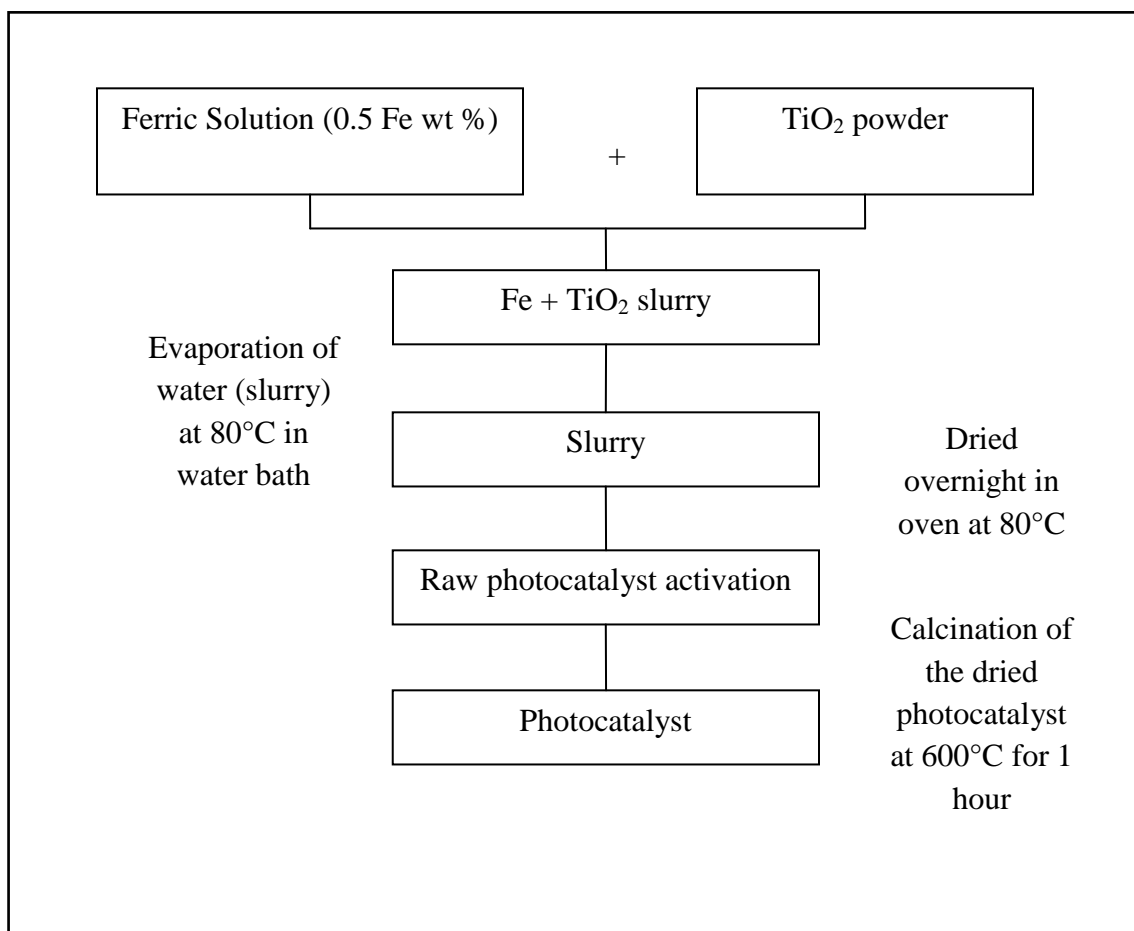


Figure 3.1: Summary of wet impregnation catalyst preparation method

3.2.2 Catalyst Characterization

Specific equipment can be used in order to find the properties of modified catalyst. Some of the equipments used in this project are listed in the table 3.2 below:

3.2.2.1 Equipments

Table 3.2: List of equipments used in this project

Equipments	Evaluate
Field Emission Scanning Electron Microscopy (FESEM)	Grain size, surface roughness, porosity, particle size distributions, material homogeneity and intermetallic distribution and diffusion.
Surface Area and Pore Size Analyzer (ASAP)	Specific surface area and pore size distribution
Thermal Gravimeter Analyzer (TGA)	Assessment of moisture, volatiles and composition, thermal and oxidative stability as well as decomposition kinetics
X-Ray Diffraction (XRD)	Crystal structure / pattern
UV-Vis Spectroscopy	Light absorption range

3.2.3 Catalyst Performance Study

The measuring key of this study is the concentration of DIPA that can be removed from the wastewater. In this experiment, some parameters will be kept constant such as:

- i. Amount of DIPA (e.g. 500 ppm)
- ii. pH (e.g. 7)
- iii. Weight of the catalyst (e.g. 0.5 g/L)
- iv. Dosage of hydrogen peroxide (e.g. 450 mg/L)

The parameters that can be varied are:

- i. Source of light (e.g. visible and UV light)

- ii. Sets of catalyst.

Catalyst performance study is conducted in a jacketed glass reactor covered with aluminium foil to avoid any hazard from UV light. A quartz tube with an 8W low pressure mercury lamp was inserted into the reactor. In this study, the degradation of DIPA is measured by observing the decreasing concentration of DIPA using High Performance Liquid Chromatography (HPLC). The standards of HPLC are as below:

Table 3.3: The standards of HPLC

Agilent 1100 HPLC	
Column	YMC Pack Polymer C18 (250 x 6.0 mm I.D.)
Eluent	60/40 of 100 mM NaH ₂ PO ₄ and 100 mM NaOH
Flowrate	1.2 mL/min
Temperature	30°C
UV detector	215 nm
Injection volume	20 µL

3.2.4 Flowchart of Experimental Procedure

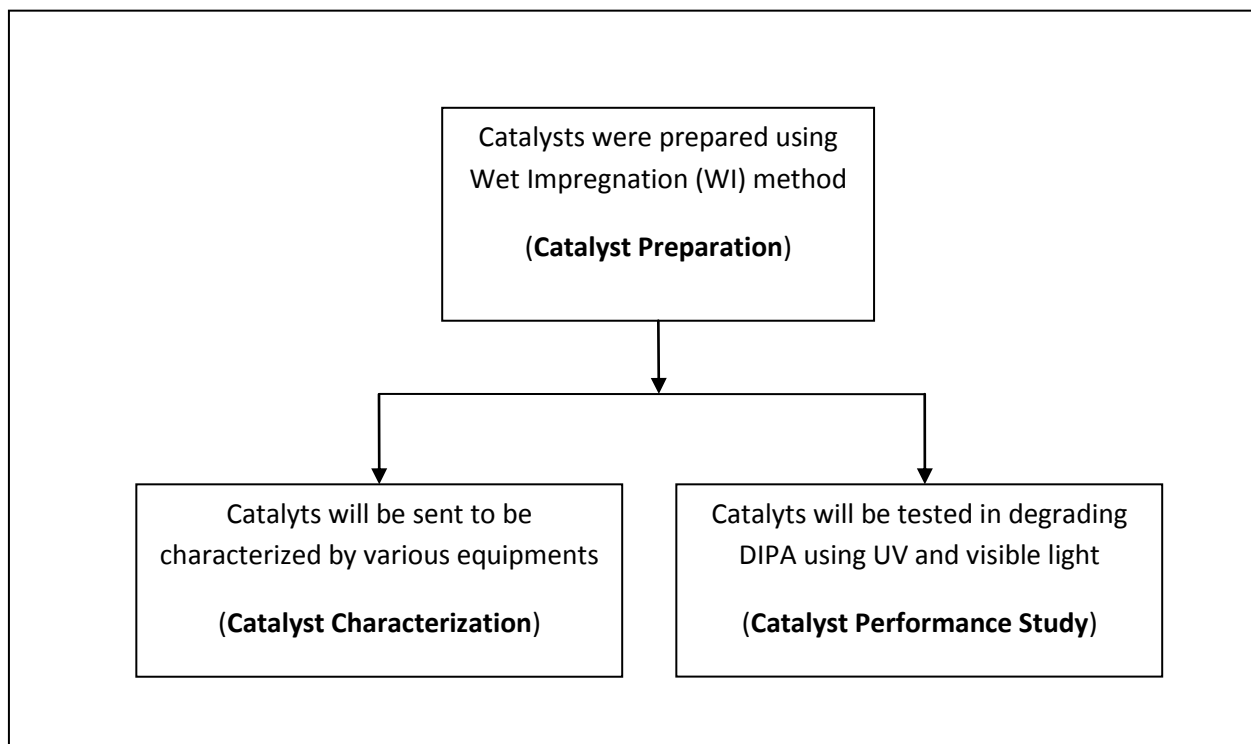


Figure 3.2: Flow chart of experimental procedure

CHAPTER 4

RESULT AND DISCUSSION

4.1 CATALYST CHARACTERIZATION

4.1.1 Thermal Gravimeter Analyzer (TGA)

Calcination is any thermal treatment carried out in order to decompose some compounds present in the catalyst, generally with evolution of gaseous products. Apart of that, the purpose of calcinations is to allow solid state reactions among different catalyst components to occur. With calcinations, all the catalysts properties, especially porous structure and mechanical strength will be induced in the degradation process later on. Thermal Gravimeter Analyzer (TGA) is important to determine the calcinations time and temperature of the catalyst. Catalysts are tested using this equipment before they are being sent into the furnace.

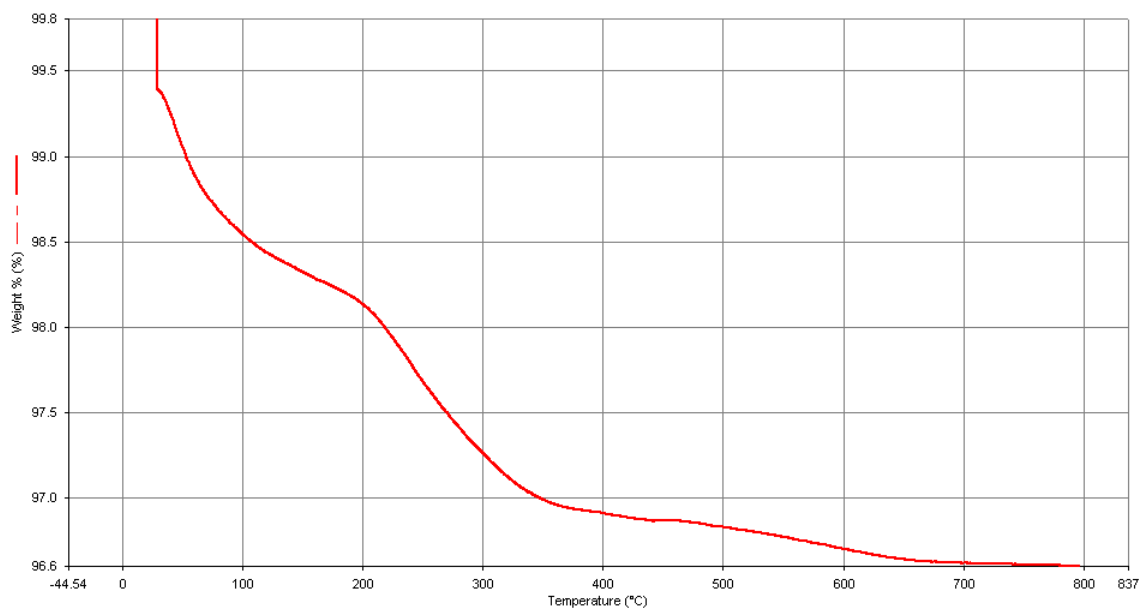


Figure 4.1: The degrading temperature of 0.3 wt% Fe catalyst

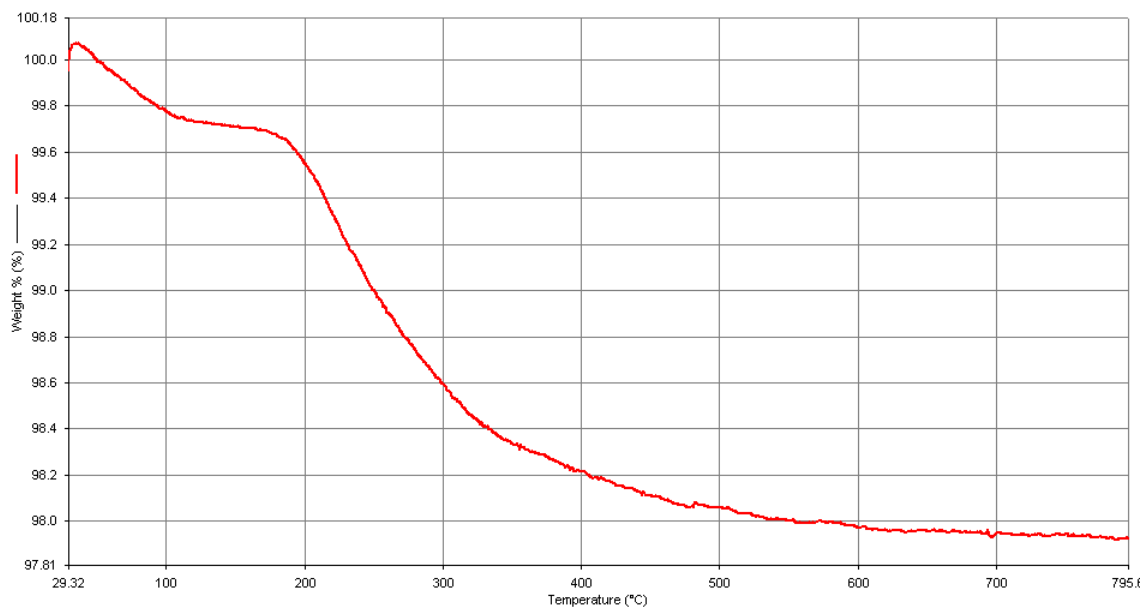


Figure 4.2: The degrading temperature of 0.7 wt% Fe catalyst

Figure 4.1 and 4.2 above shows the weight lost of the catalyst after it is dried at a certain range of temperature. From the results shown above, significant weight loss undergoes by both of the catalysts after 200°C of drying. After 700°C of drying, the catalyst has experienced complete weight lost. Therefore, the calcinations temperature of the catalyst is decided to be at 600°C and 700°C respectively. This is because, the catalyst need to be tested before and after it loss all of its component's weight completely.

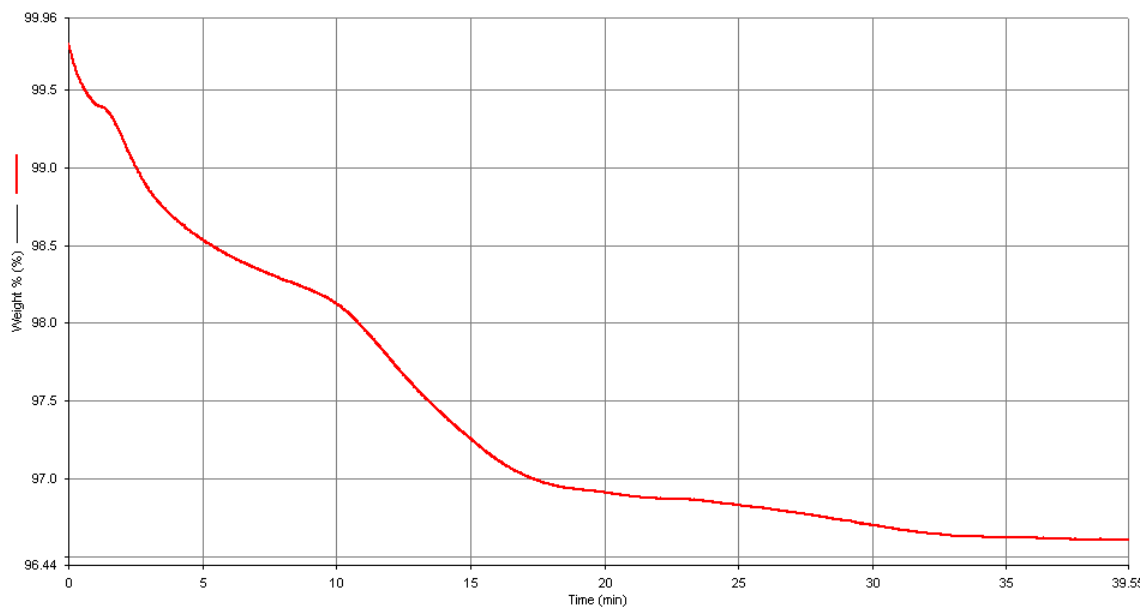


Figure 4.3: The degrading time of 0.3 wt% Fe catalyst

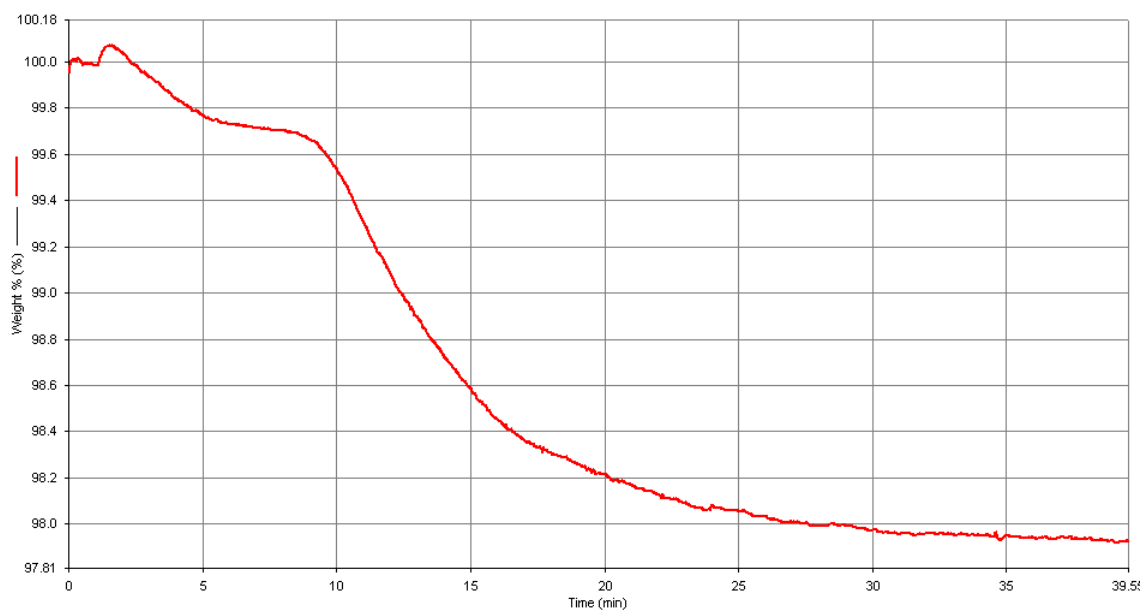


Figure 4.4: The degrading time of 0.7 wt% Fe catalyst

Figure 4.3 and 4.4 above shows the weight lost of the catalyst after it is dried at a certain range of time. From the results shown above, significant weight loss undergoes by both of the catalysts after 10 minutes of drying. After 35 min of drying, the catalyst has experienced complete weight lost. However, the calcinations time of the catalyst is decided to be at 1 and 2 hours. This is because, the normal calcinations time for catalyst containing TiO₂ particles are at 1 and 2 hours subsequently. Calcination of TiO₂

catalysts for photochemical oxidation of concentrated cholophenols under direct solar radiation is found to be optimum at 500°C for 2 hours (Ba-Abbad, M. M. et al, 2012).

4.1.2 Field Emission Scanning Electron Microscopy (FESEM)

Morphology and diameter of the particles can be seen through this equipment. These two characteristics of the particles will give some impact to the reactivity of the catalyst with the wastewater later on.

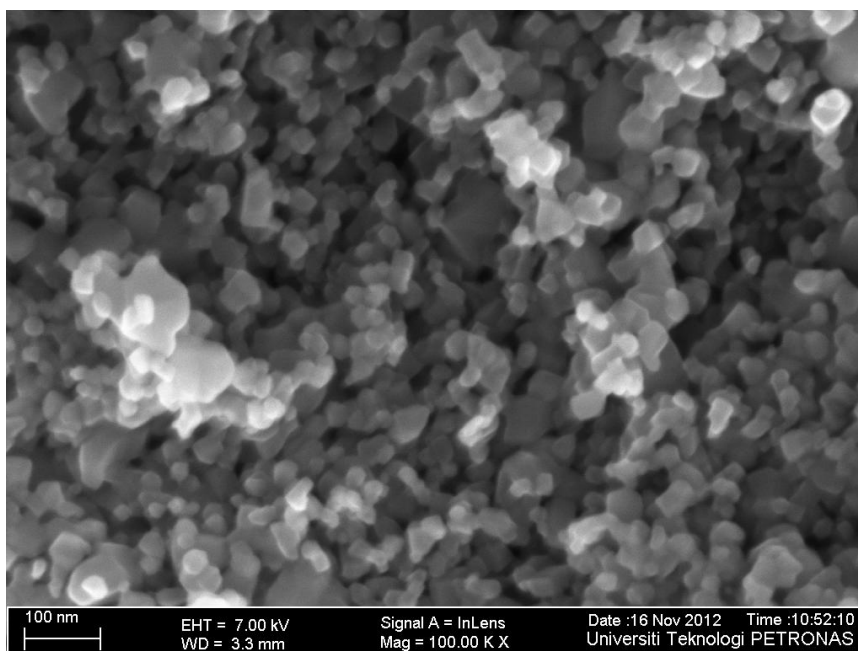


Figure 4.5: Image of 0.3 wt% Fe catalyst calcine at 600°C for 2h

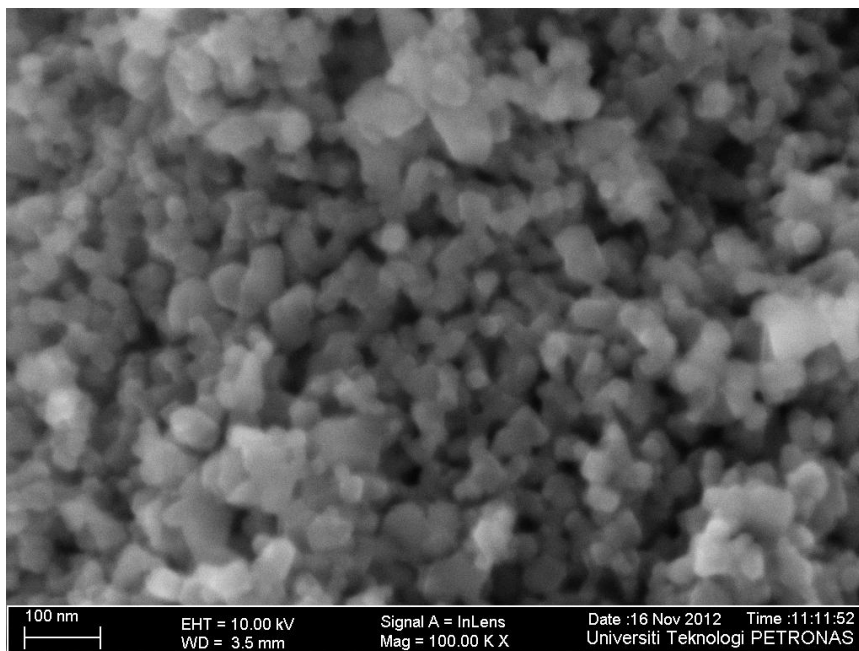


Figure 4.6: Image of 0.7 wt% Fe catalyst calcine at 600°C for 2h

The morphology of the particles of both catalysts is irregular pattern. Particles of both of the as-synthesized catalysts are approximately 3–5 μm in size. The catalyst with 0.7 wt% of Fe has larger diameter which is 3.5 μm compared to catalyst with 0.3 wt% of Fe which has diameter of 3.3 μm . With increasing weight percent of Fe, the particles form larger aggregates while morphology of the particles remains the same. Larger aggregates cause the surface area of the catalysts to be low.

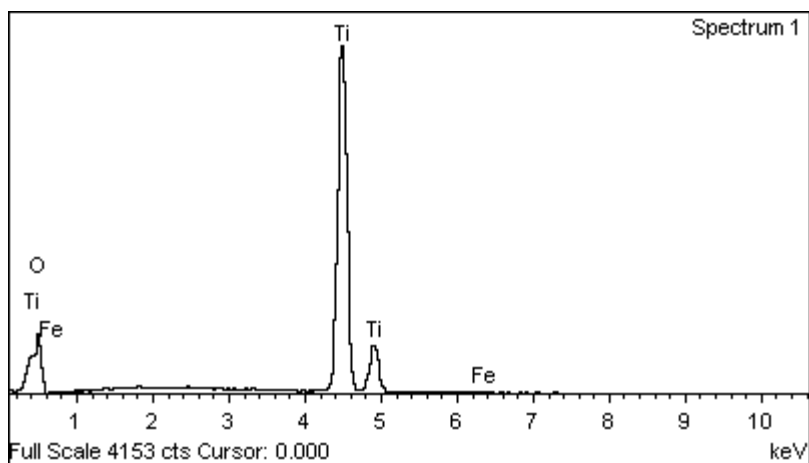


Figure 4.7: Energy dispersive X-ray spectrometry (EDX) of 0.3 wt% Fe, 600°C, 2h

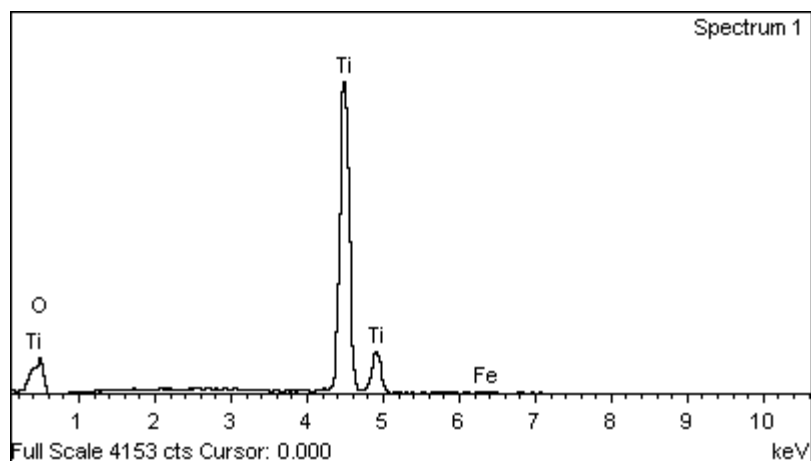


Figure 4.8: Energy dispersive X-ray spectrometry (EDX) of 0.7 wt% Fe, 600°C, 2h

Energy dispersive X-ray spectrometry (EDX) analysis of the 0.3 and 0.7 wt% Fe catalysts at 600°C shows peaks for titanium, oxygen and ferrous element. There is no trace of any other impurities could be seen within the detection limit of the EDX as presented in Figure 4.7 and 4.8.

Based on observation, 0.3 wt% Fe, 600°C, 2h catalyst has higher tendency to degrade more DIPA since it has smaller diameter of particles compared to 0.7 wt% Fe, 600°C, 2h catalyst.

4.1.3 Brunauer-Emmette-Teller (Surface Area & Porosity)

The size and number of pores determine the internal surface area. It is usually advantageous to have high surface area (large number of small pores) to maximize the dispersion of catalytic components. However, if the pore size is too small, diffusional resistance becomes a problem. BET test can give both the values of surface area and pore size of the catalysts.

Table 4.1: BET surface area of the catalysts

Catalysts	BET Surface Area (m ² g ⁻¹)
0.7 wt% Fe, 600°C, 1h	39.5713
0.7 wt% Fe, 600°C, 2h	34.2946
0.3 wt% Fe, 600°C, 1h	32.7918
0.3 wt% Fe, 600°C, 2h	30.2452
0.3 wt% Fe, 700°C, 1h	12.8040
0.3 wt% Fe, 700°C, 2h	12.3926

0.7 wt% Fe, 700°C, 1h	12.1464
0.7 wt% Fe, 700°C, 2h	11.4147

Bare TiO₂ catalysts (TiO₂ P-25 Degussa) has surface area of 63 m² g⁻¹. (Yodyingyong, S., 2011). It is shown that the synthesized TiO₂ samples is smaller than the standard sample of Degussa P-25 which is produced commercially. Catalyst that has largest surface area among all are 0.7 wt% Fe, 600°C, 1h catalyst followed by 0.7 wt% Fe, 600°C, 2h catalyst, 0.3 wt% Fe, 600°C, 1h catalyst and 0.3 wt% Fe, 600°C, 2h catalyst. This shows that the 0.7 wt% Fe, 600°C, 1h catalyst has the potential to degrade more DIPA in the wastewater.

Table 4.2: Average pore width of the catalysts

Catalysts	Average pore width (Å)
0.7 wt% Fe, 600°C, 1h	292.2111
0.7 wt% Fe, 600°C, 2h	312.7005
0.3 wt% Fe, 600°C, 1h	332.4419
0.3 wt% Fe, 600°C, 2h	337.0078
0.3 wt% Fe, 700°C, 1h	334.655
0.3 wt% Fe, 700°C, 2h	447.8332
0.7 wt% Fe, 700°C, 1h	424.6054
0.7 wt% Fe, 700°C, 2h	450.9650

The surface area of the catalyst calcined at 600°C is much lower compared to the surface area of the catalyst calcined at 700°C. Based on observation, catalyst with larger surface area has smaller pore width.

0.3 wt% Fe, 600°C, 2h catalyst has medium surface area and pore width. Thus, it can be the suitable catalyst to degrade more DIPA in the wastewater later on as it also has 3.3 μm of particle's diameter which is relatively small.

4.1.4 UV-Vis Spectroscopy

The catalysts are tested with this UV-VIS Spectrophotometer in order to determine the absorption range of the catalyst. The higher the absorptivity of the catalyst in a certain region, the higher the reactivity of the catalyst. Since the reaction of the catalyst in the

wastewater is put under the illumination of light, it is preferred to have catalyst with higher reactivity in the visible light. This is because UV light is more expensive than visible light.

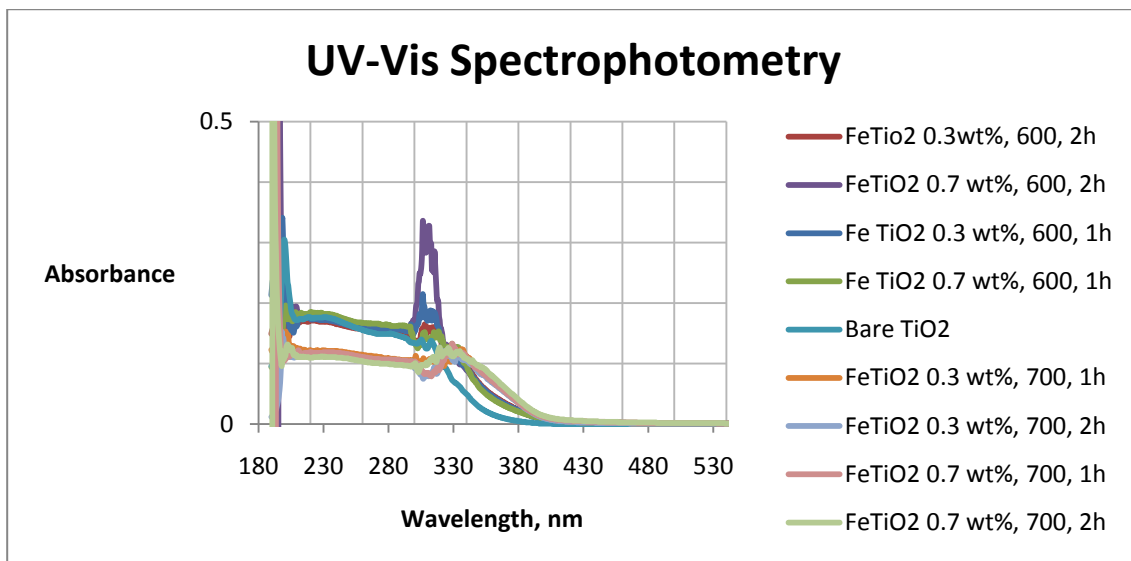


Figure 4.9: The range of wavelength of catalysts

The UV region starts from 200 to 380 nm while visible region starts from 380 to 780 nm. In UV region, all of the catalysts which have been calcined at 600°C have the absorbance of approximately 0.2. Bare TiO₂ catalyst also shows the same pattern. However, all of the catalysts that have been calcined at 700°C have the absorbance of 0.1 which is lower than the catalysts that has been calcined at 600°C. The peak of the reactivity is at 300nm. FeTiO₂ 0.7 wt%, 600°C, 2h catalyst has the highest reactivity at the peak with the absorbance of 0.32.

Meanwhile in visible region, bare TiO₂ catalysts have 0 absorbance which indicates that the catalyst is unreactive in that region. The other catalysts are slightly reactive in the visible region at the range of 380 to 400 nm. However, the catalysts which have been calcined at 600°C have the absorbance of approximately 0.13 which is lower than the catalysts that have been calcined at 700°C with the absorbance of approximately 0.14.

Since 0.7 wt%, 600°C, 2h catalyst has the highest reactivity in the UV region followed by 0.3 wt%, 600°C, 2h catalyst, it is predicted that both of the catalyst will degrade more DIPA in the wastewater compared to other catalyst.

4.2 CATALYST PERFORMANCE STUDY

The catalysts were tested in the reactor with initial concentration of DIPA at 500 ppm. The samples of the solution were taken at 30 minutes interval for two hours. This is because at two hours of reaction, the DIPA degradation process has already come to stable.

4.2.1 Reaction under UV Light

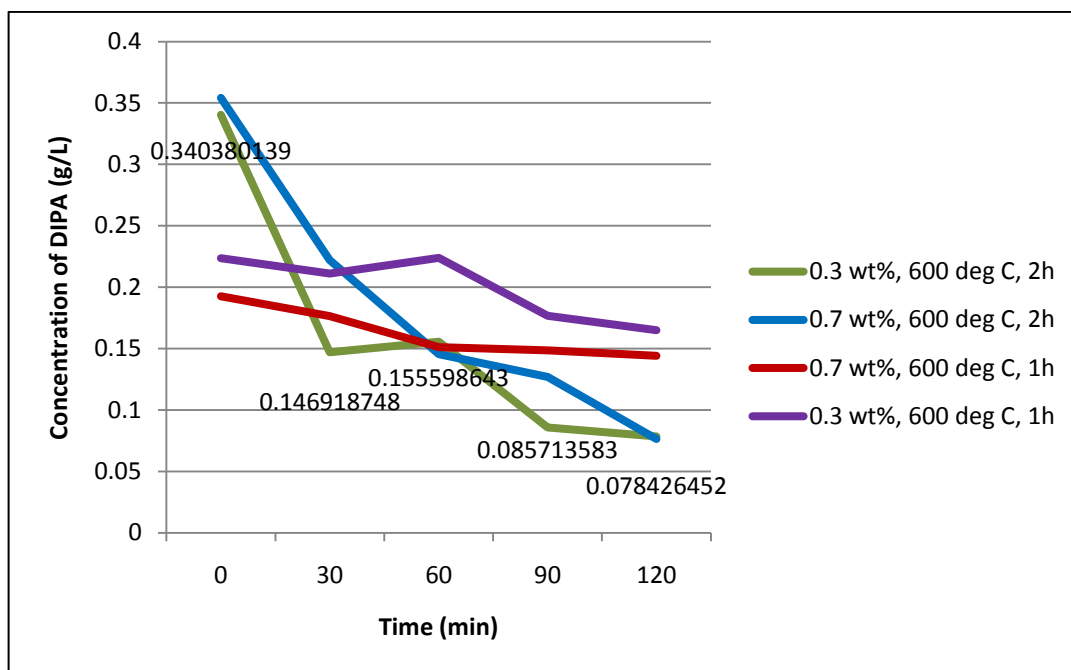


Figure 4.10: DIPA degradation rate for 0.3 and 0.7wt% of Fe catalysts calcined at 600°C for 1h and 2h under UV illumination.

Figure 4.10 shows the DIPA degradation rate for 0.3 and 0.7 wt% catalysts when they are calcined at 600°C for 1 hour and 2 hours under UV illumination. The trend shows that, 0.3 wt% catalyst calcined at 600°C for 2 hours has the best performance among all catalysts shown above. The concentration of DIPA by the catalysts reaches 0.0784 g/L after two hours of reaction.

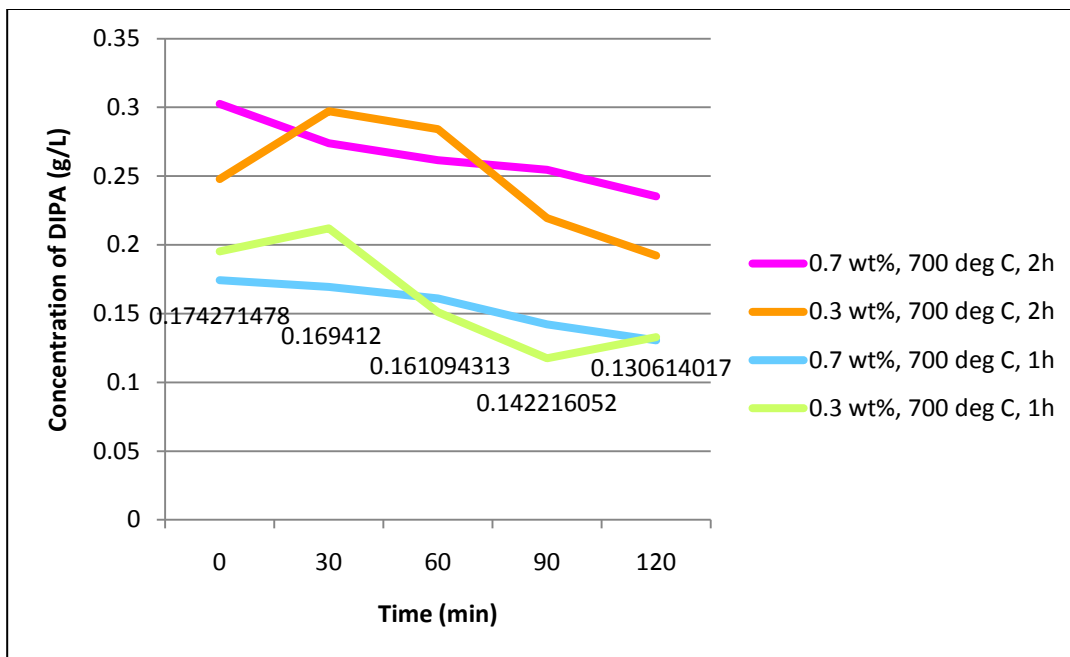


Figure 4.11: DIPA degradation rate for 0.3 and 0.7 wt% of Fe catalyst calcined at 700°C for 1h and 2h under UV illumination

Figure 4.11 shows the DIPA degradation rate for 0.3 and 0.7 wt% catalysts when they are calcined at 700°C for 1 hour and 2 hours under UV illumination. The trend shows that, 0.7 wt% catalyst calcined at 700°C for 1 hour has the best performance among all catalysts shown above. The concentration of DIPA by the catalysts reaches 0.1306 g/L after two hours of reaction.

4.2.1 Reaction under Visible Light

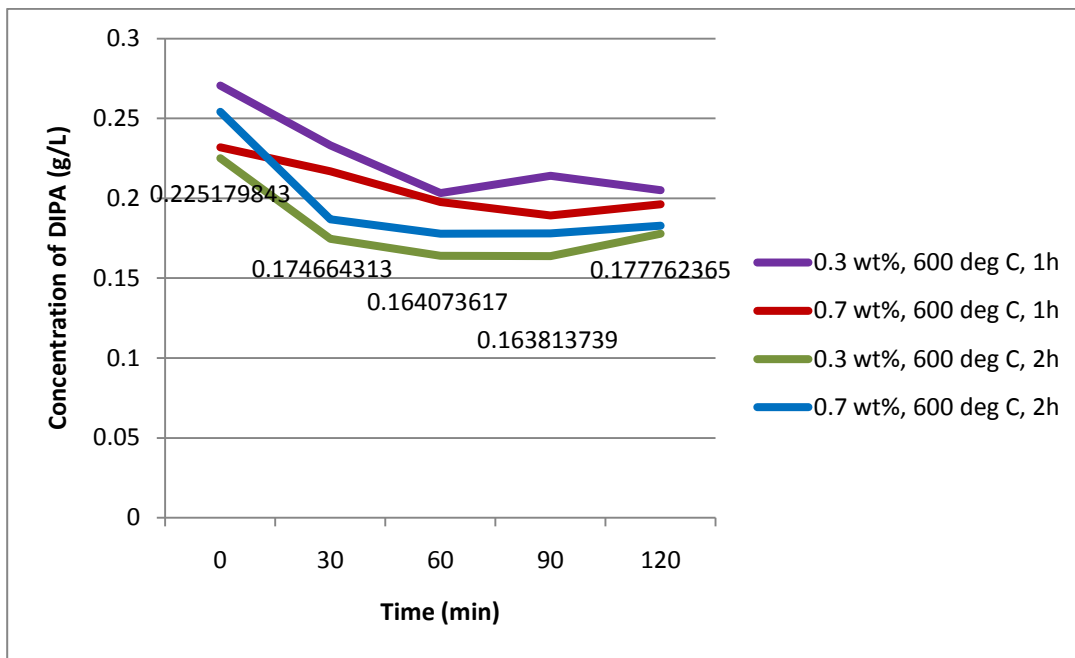


Figure 4.12: DIPA degradation rate for 0.3 and 0.7 wt% of Fe catalyst calcined at 600°C for 1h and 2h under visible illumination

Figure 4.12 shows the DIPA degradation rate for 0.3 and 0.7 wt% catalysts when they are calcined at 600°C for 1 hour and 2 hours under visible illumination. The trend shows that, 0.3 wt% catalyst calcined at 600°C for 2 hours has the best performance among all catalysts shown above. The concentration of DIPA by the catalysts reaches 0.1638 g/L after one and a half hours of reaction.

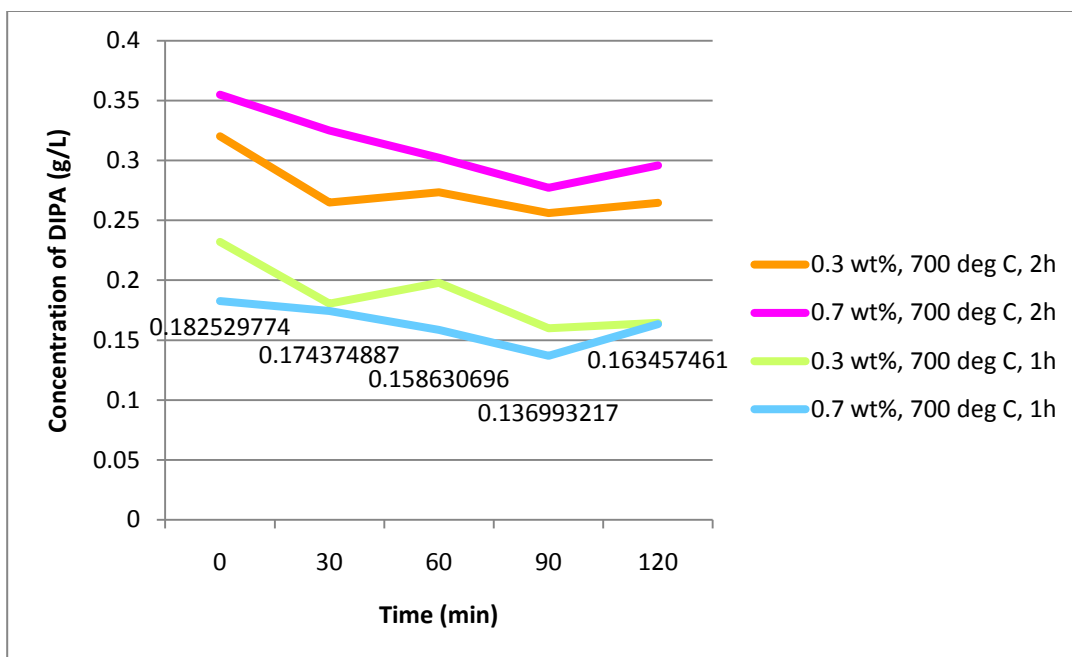


Figure 4.13: DIPA degradation rate for 0.3 and 0.7 wt% of Fe catalyst calcined at 700°C for 1h and 2h under visible illumination

Figure 4.13 shows the DIPA degradation rate for 0.3 and 0.7 wt% catalysts when they are calcined at 700°C for 1 hour and 2 hours under visible illumination. The trend shows that, 0.7 wt% catalyst calcined at 700°C for 1 hour has the best performance among all catalysts shown above. The concentration of DIPA by the catalysts reaches 0.1370 g/L after one and a half hours of reaction.

Based on observation, the lower the weight percent of Fe, the lower the concentration of DIPA in wastewater after 2 hours of reaction. However, it depends on the calcinations temperature and time of the catalysts. The catalysts that have been calcined for 1 hour produce better results than catalysts that have been calcined for 2 hours. This is because, with increasing calcinations time, the particle size of the catalyst also will increase. Increasing particle size will cause the surface area to be smaller. This is the same with calcinations temperature. As the temperature increase, the particle size of the catalyst also will increase. (Yodyingyong, S., 2011).

In conclusion, 0.3 wt%, 600°C, 2h catalyst has proven to be reactive in both UV and visible region among other catalyst that have been calcined at 600°C. On the other hand, 0.7 wt%, 700°C, 1h catalyst has proven to be reactive in both UV and visible region

among other catalyst that has been calcined at 700°C. However, 0.3 wt%, 600°C, 2h catalyst has high reactivity in the UV region since it has degrade DIPA until it reaches 0.0784 g/L of concentration. Therefore, 0.3 wt%, 600°C, 2h catalyst emerged as the best catalyst among all.

CHAPTER 5

CONCLUSIONS AND RECOMMENDATION

5.1 CONCLUSION

5.1.1 Catalyst Preparation

A total of eight catalysts with different calcinations time, temperature and Fe weight percent have been prepared. These catalysts were prepared using the wet impregnation method.

5.1.2 Catalyst Characterization

5.1.2.1 *Thermal Gravimeter Analyzer (TGA)*

After drying the catalyst in the oven, few catalysts are tested using this equipment to determine the calcinations time and temperature. The calcinations time of the catalysts are decided to be at 1 and 2 hours respectively while the calcinations temperature of the catalysts are decided to be at 600°C and 700°C respectively.

5.1.2.2 *Field Emission Scanning Electron Microscopy (FESEM)*

The morphology of the particles of both catalysts is irregular pattern. The catalyst with 0.7 wt% of Fe has larger diameter which is 3.5 μm compared to catalyst with 0.3 wt% of Fe which has diameter of 3.3 μm .

5.1.2.3 *Brunauer-Emmette-Teller (Surface Area & Porosity)*

Catalyst with larger surface area have smaller pore sizes. Since the catalyst are better with larger size of both of the properties, average values of surface area and pore sizes can be found in 0.3 wt%, 600°C, 2h catalyst. Therefore, the catalyst emerged as the winner among all other catalyst.

5.1.2.4 UV-Vis Spectroscopy

All catalysts that have been prepared are more reactive in UV region including bare TiO₂ catalyst. However, in visible region, bare TiO₂ is not reactive at all compared to other catalysts which are slightly reactive at the range of 380 to 400 nm.

5.1.2 Catalyst Performance Study

0.3 wt% catalyst calcined at 600°C for 2 hours give the best performance in degrading DIPA under the illumination of both UV and visible light. On the other hand, 0.7 wt% catalyst is better in both UV and visible light when it is calcined for 1 hour at 700°C. However, 0.3 wt% catalyst calcined at 600°C for 2 hours is much preferred as it gives lower DIPA concentration after two hours of reaction which is 0.0784 g/L.

5.2 RECOMMENDATION

- 1) X-ray Diffraction (XRD) test can be performed on the catalyst to find out the phase of the catalyst whether it is in rutile or anatase phase. Apart of that, and study of zero point of charge is worth to find out whether the catalyst posses the same or different charge with DIPA.
- 2) Producing catalyst in smaller quantity tends to give more accurate result in terms of characterization. Thus, it is recommended to produce the catalyst in smaller scale at one time.
- 3) Catalyst preparation method can be compared before deciding which method to be used in order to produce better catalyst. For example, co-precipitation method can be compared with wet impregnation method.
- 4) In order to save time, the author only makes two hours of reaction of the catalyst with DIPA. The reaction can be prolonged to three hours and above to observe a more stable DIPA degradation reaction.
- 5) Higher concentration of initial DIPA is preferred before carrying out the reaction. This is because, the HPLC will not be able to detect below than 100 ppm of DIPA after degradation process took place.

REFERENCES

- [1] *Processing natural gas*. Retrieved June, 2012, from NaturalGas.org
- [2] Kohl, A. I., & Nielsen, R. B. (1997). Gas purification. *Gulf Publishing Company, Houston, Texas*.
- [3] J. C. Lou & S. S. Lee (1995). Chemical oxidation of BTX using Fenton's reagent. *Journal of Hazardous Material*, 12, 185-195.
- [4] Goi, A., & Trapido, M. (2002). Hydrogen peroxide photolysis, fenton's reagent and photo-fenton for the degradation of nitrophenols: A comparative study. *Canadian Journal on Chemical Engineering and Technology*, 46, 913-922.
- [5] I. Gulkaya, G. A. Surucu, & F. B. Dilek (2006). Importance of H_2O_2/Fe^{2+} ration in Fenton's treatment of a carpet dyeing wastewater. *Journal of Hazardous Material*, B136, 763-769.
- [6] Matthew, A. T. (2003). Fenton and modified fenton methods for pollutant degradation. *Chemical Degradation Methods for Wastes and Pollutants*, 30.
- [7] Sabtanti, H., Dutta, B. K., Idzham, F. M., Chakrabarti, S., & Vione, D. (2009). Degradation of monoethanolamine in aqueous solution by fenton's reagent with biological post-treatment. *Water, Air and Soil Pollution*, 211, 273-286.
- [8] Dutta, B. K., Sabtanti, H., Idzham, F. M., Chakrabarti, S., & Vione, D. (2010). Degradation of diethanolamine by fenton's reagent combined with biological post treatment. *Desalination and Water Treatment*, 19, 286-293.
- [9] Omar, A. A., Raihan, M. R., & Putri, N. F. (2010). Fenton oxidation of natural gas plant wastewater. *Canadian Journal on Chemical Engineering and Technology*, 1, 1-6.

- [10] Vinita, M., Praveena, J. D., & Palanivelu, K. (2010). Degradation of 2,4,6-trichlorophenol by photo fenton's like method using nano heterogeneous catalytic ferric ion. *Solar Energy*, 84, 1613-1618.
- [11] Zhang, Y., Fengzhu, L., Tao, W., Li, Y., Zhang, R., Shen, B., Paul, K. C. (2011). F and fe co-doped TiO₂ with enhanced visible light photocatalytic activity. 59, 387-391.
- [12] C. Adan, J. Carbajo, A. Bahamonde, A. Martinez-Arias (2009). Phenol photodegradation with oxygen and hydrogen peroxide over TiO₂ and Fe-doped TiO₂. *Catalysis Today*, 143, 247-252.
- [13] M. Asilturk, F. Sayilkan, E. Arpac (2009). Effect of Fe³⁺ ion doping to TiO₂ on the photocatalytic degradation of Malachite Green dye under UV and vis-irradiation. *Journal of Photochemistry and Photobiology A Chemistry*, 203, 64-71.
- [14] N. Banic, B. Abramovic, J. Krstic, D. Sojic, L. Davor, Z. Cherkezova-Zheleva, V. Guzsvany (2011). Photodegradation of thiacloprid using Fe/TiO₂ as a heterogeneous photo-Fenton catalyst. *Applied Catalyst B: Environmental*, 107, 363-371.
- [15] Klare, M., Scheen, J., Vogelsang, K., Jacobs, H., & Broekaert, J. A. (2000). Degradation of short-chain alkyl- and alkanolamines by TiO₂- and Pt/TiO₂-assisted photocatalysis. 41, 353-362.
- [16] C. S. Lu, C. C. Chen, F. D. Mai, H. K. Li (2009). Identification of the degradation pathways of alkanolamines with TiO₂ photocatalysis. *Journal of Hazardous Materials*, 165, 306-316.
- [17] Khan, M. A., Seong, I. W., & Yang, O. B. (2008). Hydrothermally stabilized fe(III) doped titania active under visible light for water splitting reaction. *International Journal of Hydrogen Energy*, 33, 5345-5351.

- [18] Environmental quality (sewage and industrial effluents) regulation 1979. (1974).
M. Department of Environment, Environmental Quality Act (EQA).
- [19] Ba-Abbad, M. M., Khadum, A. A. H., Mohamad, A. B., Takriff, M. S., Soppian, K. (2012). Synthesize and Catalytic activity of TiO₂ Nanoparticles for Photochemical Oxidation of Concentrated Chlorophenols under Direct Solar Radiation. *International Journal of Electrochemical Science*, 7, 4871-4888.
- [20] Yodyingyong, S., Sae-Kyung, C., Panjipan, B., Triampo, W., Traimpo, D. (2011). Physicochemical properties of nanoparticles titania from alcohol burner calcinations. *Chemical Society of Ethiopia*, 25(2), 263-272.

APPENDICES

Sample: 000-146 J123/SAP/11/12 0.3, 700 1hr
Operator: Omar
Submitter: Adnin
File: C:\WIN3020\DATA\000-146.SMP

Started: 5/12/2012 5:15:45PM
Completed: 6/12/2012 2:03:23AM
Report Time: 7/12/2012 3:12:14PM
Warm Free Space: 20.4785 cm³ Measured
Equilibration Interval: 10 s
Sample Density: 1.000 g/cm³

Analysis Adsorptive: N2
Analysis Bath Temp.: -195.800 °C
Sample Mass: 0.3094 g
Cold Free Space: 57.1260 cm³ Measured
Low Pressure Dose: None
Automatic Degas: Yes

Sample Prep: Stage	Temperature (°C)	Ramp Rate (°C/min)	Time (min)
1	90	10	30
2	300	10	240

Summary Report

Surface Area

Single point surface area at $p/p^0 = 0.299403648$: 12.2951 m²/g

BET Surface Area: 12.8040 m²/g

Langmuir Surface Area: 20.2766 m²/g

t-Plot External Surface Area: 15.9431 m²/g

BJH Adsorption cumulative surface area of pores
between 17.000 Å and 3000.000 Å diameter: 14.494 m²/g

BJH Desorption cumulative surface area of pores
between 17.000 Å and 3000.000 Å diameter: 15.1331 m²/g

Pore Volume

t-Plot micropore volume: -0.001785 cm³/g

BJH Adsorption cumulative volume of pores
between 17.000 Å and 3000.000 Å diameter: 0.121260 cm³/g

BJH Desorption cumulative volume of pores
between 17.000 Å and 3000.000 Å diameter: 0.120087 cm³/g

Pore Size

BJH Adsorption average pore diameter (4V/A): 334.655 Å

BJH Desorption average pore diameter (4V/A): 317.417 Å

Sample: 000-148 J123/SAP/11/12 0.3, 700 2hr
Operator: Omar
Submitter: Adnin
File: C:\WIN3020\DATA\000-148.SMP

Started: 5/12/2012 5:15:45PM	Analysis Adsorptive: N2
Completed: 6/12/2012 2:03:23AM	Analysis Bath Temp.: -195.800 °C
Report Time: 7/12/2012 3:12:15PM	Sample Mass: 0.3001 g
Warm Free Space: 20.6054 cm ³ Measured	Cold Free Space: 57.6062 cm ³ Measured
Equilibration Interval: 10 s	Low Pressure Dose: None
Sample Density: 1.000 g/cm ³	Automatic Degas: Yes

Sample Prep: Stage	Temperature (°C)	Ramp Rate (°C/min)	Time (min)
1	90	10	30
2	300	10	240

Summary Report

Surface Area

Single point surface area at $p/p^{\circ} = 0.299391050$: 11.8702 m²/g

BET Surface Area: 12.3926 m²/g

Langmuir Surface Area: 19.7391 m²/g

t-Plot External Surface Area: 15.7849 m²/g

BJH Adsorption cumulative surface area of pores
between 17.000 Å and 3000.000 Å diameter: 14.185 m²/g

BJH Desorption cumulative surface area of pores
between 17.000 Å and 3000.000 Å diameter: 14.9320 m²/g

Pore Volume

Single point adsorption total pore volume of pores
less than 0.000 Å diameter at $p/p^{\circ} = 1.000189711$: 0.138745 cm³/g

t-Plot micropore volume: -0.001932 cm³/g

BJH Adsorption cumulative volume of pores
between 17.000 Å and 3000.000 Å diameter: 0.118583 cm³/g

BJH Desorption cumulative volume of pores
between 17.000 Å and 3000.000 Å diameter: 0.128048 cm³/g

Pore Size

Adsorption average pore width (4V/A by BET): 447.8332 Å

BJH Adsorption average pore diameter (4V/A): 334.395 Å

BJH Desorption average pore diameter (4V/A): 343.016 Å

Sample: 000-145 J123/SAP/11/12 0.7-700-1hr
Operator: Omar
Submitter: Adnin
File: C:\WIN3020\DATA\000-145.SMP

Started: 4/12/2012 8:30:53AM	Analysis Adsorptive: N2
Completed: 4/12/2012 6:20:14PM	Analysis Bath Temp.: -195.800 °C
Report Time: 7/12/2012 3:12:13PM	Sample Mass: 0.2979 g
Warm Free Space: 20.7290 cm ³ Measured	Cold Free Space: 59.0572 cm ³ Measured
Equilibration Interval: 10 s	Low Pressure Dose: None
Sample Density: 1.000 g/cm ³	Automatic Degas: Yes

Sample Prep: Stage	Temperature (°C)	Ramp Rate (°C/min)	Time (min)
1	90	10	30
2	300	10	240

Summary Report

Surface Area

Single point surface area at $p/p^{\circ} = 0.299349782$: 11.7178 m²/g

BET Surface Area: 12.1464 m²/g

Langmuir Surface Area: 19.1743 m²/g

t-Plot External Surface Area: 14.8496 m²/g

BJH Adsorption cumulative surface area of pores
between 17.000 Å and 3000.000 Å diameter: 14.030 m²/g

BJH Desorption cumulative surface area of pores
between 17.000 Å and 3000.000 Å diameter: 14.2916 m²/g

Pore Volume

Single point adsorption total pore volume of pores
less than 23287.910 Å diameter at $p/p^{\circ} = 0.999177336$: 0.128936 cm³/g

t-Plot micropore volume: -0.001551 cm³/g

BJH Adsorption cumulative volume of pores
between 17.000 Å and 3000.000 Å diameter: 0.128712 cm³/g

BJH Desorption cumulative volume of pores
between 17.000 Å and 3000.000 Å diameter: 0.123132 cm³/g

Pore Size

Adsorption average pore width (4V/A by BET): 424.6054 Å

BJH Adsorption average pore diameter (4V/A): 366.951 Å

BJH Desorption average pore diameter (4V/A): 344.628 Å

Sample: 000-147 J123/SAP/11/12 0.7, 700 2hr
Operator: Omar
Submitter: Adnin
File: C:\WIN3020\DATA\000-147.SMP

Started: 5/12/2012 5:15:45PM Analysis Adsorptive: N2
Completed: 6/12/2012 2:03:23AM Analysis Bath Temp.: -195.800 °C
Report Time: 7/12/2012 3:12:15PM Sample Mass: 0.2958 g
Warm Free Space: 20.5866 cm³ Measured Cold Free Space: 57.8012 cm³ Measured
Equilibration Interval: 10 s Low Pressure Dose: None
Sample Density: 1.000 g/cm³ Automatic Degas: Yes

Sample Prep: Stage	Temperature (°C)	Ramp Rate (°C/min)	Time (min)
1	90	10	30
2	300	10	240

Summary Report

Surface Area

Single point surface area at $p/p^{\circ} = 0.299678079$: 10.9765 m²/g

BET Surface Area: 11.4147 m²/g

Langmuir Surface Area: 18.0120 m²/g

t-Plot External Surface Area: 13.7862 m²/g

BJH Adsorption cumulative surface area of pores
between 17.000 Å and 3000.000 Å diameter: 12.761 m²/g

BJH Desorption cumulative surface area of pores
between 17.000 Å and 3000.000 Å diameter: 12.4786 m²/g

Pore Volume

Single point adsorption total pore volume of pores
less than 25209.214 Å diameter at $p/p^{\circ} = 0.999240228$: 0.128691 cm³/g

t-Plot micropore volume: -0.001363 cm³/g

BJH Adsorption cumulative volume of pores
between 17.000 Å and 3000.000 Å diameter: 0.128332 cm³/g

BJH Desorption cumulative volume of pores
between 17.000 Å and 3000.000 Å diameter: 0.124240 cm³/g

Pore Size

Adsorption average pore width (4V/A by BET): 450.9650 Å

BJH Adsorption average pore diameter (4V/A): 402.278 Å

BJH Desorption average pore diameter (4V/A): 398.250 Å

Sample: 000-631 J190/SAP/11/12 0.3wt% WI600C 1hr
Operator: Omar
Submitter: Adnin
File: C:\2020\DATA\NOVEMB~1\000-631.SMP

Started: 11/21/2012 9:51:19AM	Analysis Adsorptive: N2
Completed: 11/21/2012 7:34:50PM	Analysis Bath Temp.: -195.860 °C
Report Time: 12/7/2012 3:03:46PM	Thermal Correction: No
Sample Mass: 0.2871 g	Warm Free Space: 28.0938 cm ³ Measured
Cold Free Space: 86.0416 cm ³	Equilibration Interval: 10 s
Low Pressure Dose: None	Automatic Degas: Yes

Notes:

Summary Report

Surface Area

Single point surface area at P/Po = 0.249484001: 31.8508 m²/g

BET Surface Area: 32.7918 m²/g

Langmuir Surface Area: 48.6968 m²/g

t-Plot Micropore Area: 0.6363 m²/g

t-Plot External Surface Area: 32.1555 m²/g

BJH Adsorption cumulative surface area of pores
between 17.000 Å and 3000.000 Å width: 34.893 m²/g

BJH Desorption cumulative surface area of pores
between 17.000 Å and 3000.000 Å width: 39.0510 m²/g

Pore Volume

Single point adsorption total pore volume of pores
less than 1425.334 Å width at P/Po = 0.986234148: 0.272534 cm³/g

Single point desorption total pore volume of pores
less than 987.666 Å width at P/Po = 0.979997067: 0.287648 cm³/g

t-Plot micropore volume: -0.000060 cm³/g

BJH Adsorption cumulative volume of pores
between 17.000 Å and 3000.000 Å width: 0.295558 cm³/g

BJH Desorption cumulative volume of pores
between 17.000 Å and 3000.000 Å width: 0.294931 cm³/g

Pore Size

Adsorption average pore width (4V/A by BET): 332.4419 Å

Desorption average pore width (4V/A by BET): 350.8784 Å

BJH Adsorption average pore width (4V/A): 338.819 Å

BJH Desorption average pore width (4V/A): 302.098 Å

Sample: 000-633 J190/SAP/11/12 0.3wt% Wi 600C 2hr
Operator: Omar
Submitter: Adnin
File: C:\2020\DATA\NOVEMB~1\000-633.SMP

Started: 11/23/2012 9:52:54AM	Analysis Adsorptive: N2
Completed: 11/23/2012 6:28:00PM	Analysis Bath Temp.: -195.841 °C
Report Time: 12/7/2012 3:03:49PM	Thermal Correction: No
Sample Mass: 0.2994 g	Warm Free Space: 28.0859 cm ³ Measured
Cold Free Space: 86.0703 cm ³	Equilibration Interval: 10 s
Low Pressure Dose: None	Automatic Degas: Yes

Summary Report

Surface Area

Single point surface area at P/Po = 0.249166786: 29.3496 m²/g

BET Surface Area: 30.2452 m²/g

Langmuir Surface Area: 44.9787 m²/g

t-Plot Micropore Area: 0.0152 m²/g

t-Plot External Surface Area: 30.2300 m²/g

BJH Adsorption cumulative surface area of pores
between 17.000 Å and 3000.000 Å width: 34.863 m²/g

BJH Desorption cumulative surface area of pores
between 17.000 Å and 3000.000 Å width: 39.1456 m²/g

Pore Volume

Single point adsorption total pore volume of pores
less than 3326.707 Å width at P/Po = 0.994169821: 0.254821 cm³/g

Single point desorption total pore volume of pores
less than 823.590 Å width at P/Po = 0.975918486: 0.252047 cm³/g

t-Plot micropore volume: -0.000357 cm³/g

BJH Adsorption cumulative volume of pores
between 17.000 Å and 3000.000 Å width: 0.255497 cm³/g

BJH Desorption cumulative volume of pores
between 17.000 Å and 3000.000 Å width: 0.254983 cm³/g

Pore Size

Adsorption average pore width (4V/A by BET): 337.0078 Å

Desorption average pore width (4V/A by BET): 333.3380 Å

BJH Adsorption average pore width (4V/A): 293.141 Å

BJH Desorption average pore width (4V/A): 260.548 Å

Sample: 000-632 J190/SAP/11/12 0.7wt% WI600C 1hr
Operator:
Submitter:
File: C:\2020\DATA\NOVEMB~1\000-632.SMP

Started: 11/22/2012 9:30:21AM	Analysis Adsorptive: N2
Completed: 11/22/2012 7:42:25PM	Analysis Bath Temp.: -195.856 °C
Report Time: 12/7/2012 3:03:48PM	Thermal Correction: No
Sample Mass: 0.3024 g	Warm Free Space: 27.8931 cm ³ Measured
Cold Free Space: 85.1872 cm ³	Equilibration Interval: 10 s
Low Pressure Dose: None	Automatic Degas: Yes

Summary Report

Surface Area

Single point surface area at P/Po = 0.249716321: 38.2879 m²/g

BET Surface Area: 39.5713 m²/g

Langmuir Surface Area: 58.9580 m²/g

t-Plot External Surface Area: 40.0752 m²/g

BJH Adsorption cumulative surface area of pores
between 17.000 Å and 3000.000 Å width: 42.854 m²/g

BJH Desorption cumulative surface area of pores
between 17.000 Å and 3000.000 Å width: 47.3661 m²/g

Pore Volume

Single point adsorption total pore volume of pores
less than 1153.516 Å width at P/Po = 0.982925440: 0.289080 cm³/g

Single point desorption total pore volume of pores
less than 859.825 Å width at P/Po = 0.976955321: 0.317303 cm³/g

t-Plot micropore volume: -0.000731 cm³/g

BJH Adsorption cumulative volume of pores
between 17.000 Å and 3000.000 Å width: 0.322876 cm³/g

BJH Desorption cumulative volume of pores
between 17.000 Å and 3000.000 Å width: 0.322147 cm³/g

Pore Size

Adsorption average pore width (4V/A by BET): 292.2111 Å

Desorption average pore width (4V/A by BET): 320.7404 Å

BJH Adsorption average pore width (4V/A): 301.375 Å

BJH Desorption average pore width (4V/A): 272.048 Å

Sample: 000-634 J190/SAP/11/12 0.7wt% Wi 600C 2hr
Operator: Omar
Submitter: Adnin
File: C:\2020\DATA\NOVEMB~1\000-634.SMP

Started: 11/24/2012 8:59:54AM	Analysis Adsorptive: N2
Completed: 11/24/2012 6:34:28PM	Analysis Bath Temp.: -195.829 °C
Report Time: 12/7/2012 3:03:51PM	Thermal Correction: No
Sample Mass: 0.2915 g	Warm Free Space: 28.2443 cm ³ Measured
Cold Free Space: 85.7645 cm ³	Equilibration Interval: 10 s
Low Pressure Dose: None	Automatic Degas: Yes

Summary Report

Surface Area

Single point surface area at P/Po = 0.249720890: 32.8433 m²/g

BET Surface Area: 34.2946 m²/g

Langmuir Surface Area: 51.6539 m²/g

t-Plot External Surface Area: 37.3565 m²/g

BJH Adsorption cumulative surface area of pores
between 17.000 Å and 3000.000 Å width: 39.891 m²/g

BJH Desorption cumulative surface area of pores
between 17.000 Å and 3000.000 Å width: 42.7572 m²/g

Pore Volume

Single point adsorption total pore volume of pores
less than 1228.294 Å width at P/Po = 0.983983752: 0.268098 cm³/g

Single point desorption total pore volume of pores
less than 871.925 Å width at P/Po = 0.977282047: 0.293298 cm³/g

t-Plot micropore volume: -0.002026 cm³/g

BJH Adsorption cumulative volume of pores
between 17.000 Å and 3000.000 Å width: 0.298923 cm³/g

BJH Desorption cumulative volume of pores
between 17.000 Å and 3000.000 Å width: 0.297891 cm³/g

Pore Size

Adsorption average pore width (4V/A by BET): 312.7005 Å

Desorption average pore width (4V/A by BET): 342.0925 Å

BJH Adsorption average pore width (4V/A): 299.742 Å

BJH Desorption average pore width (4V/A): 278.681 Å

Spectrum processing :

No peaks omitted

Processing option : All elements analyzed (Normalised)

Number of iterations = 4

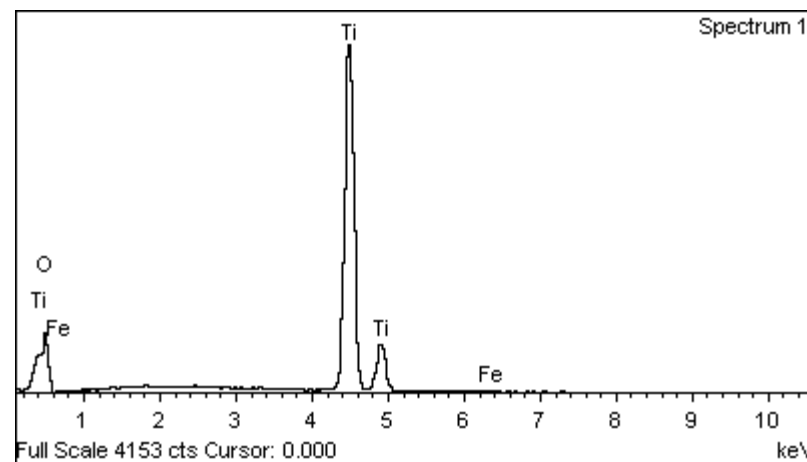
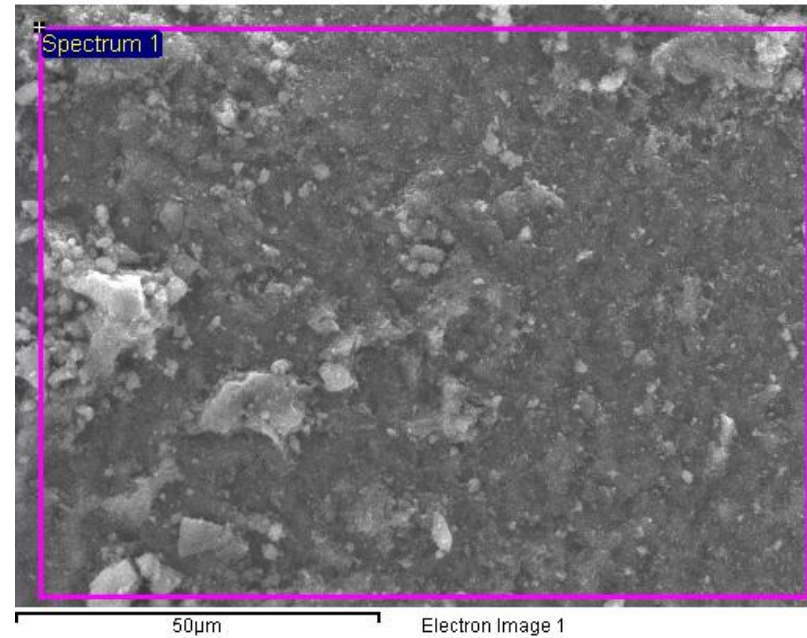
Standard :

O SiO2 1-Jun-1999 12:00 AM

Ti Ti 1-Jun-1999 12:00 AM

Fe Fe 1-Jun-1999 12:00 AM

Element	Weight%	Atomic%
O K	44.18	70.34
Ti K	55.39	29.46
Fe K	0.44	0.20
Totals	100.00	



Comment:

Spectrum processing :

No peaks omitted

Processing option : All elements analyzed (Normalised)

Number of iterations = 3

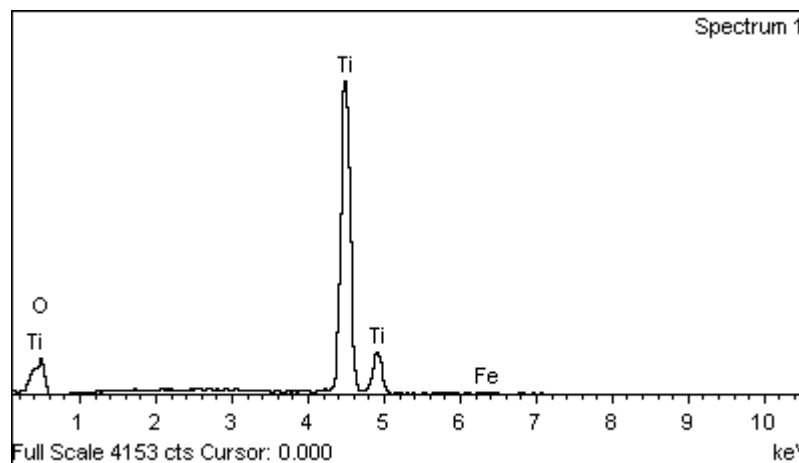
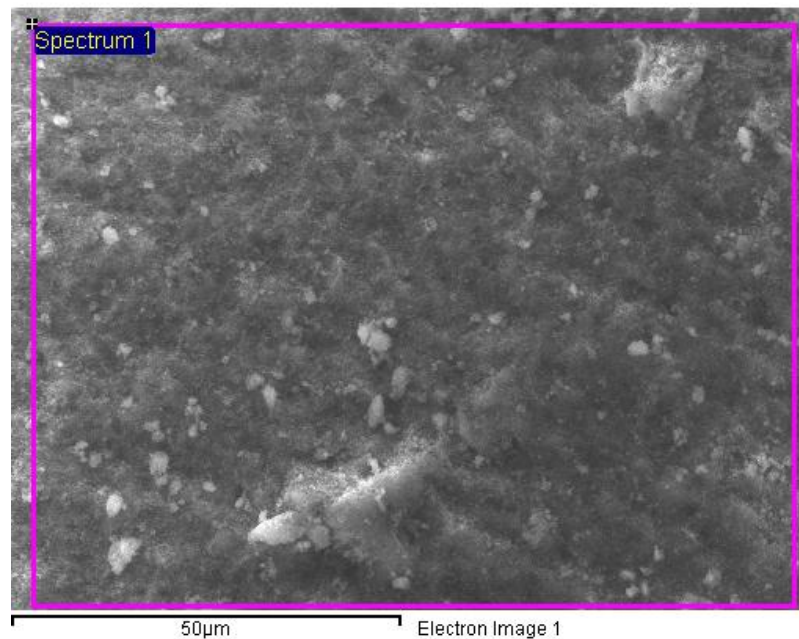
Standard :

O SiO2 1-Jun-1999 12:00 AM

Ti Ti 1-Jun-1999 12:00 AM

Fe Fe 1-Jun-1999 12:00 AM

Element	Weight%	Atomic%
O K	38.47	65.21
Ti K	60.96	34.51
Fe K	0.58	0.28
Totals	100.00	

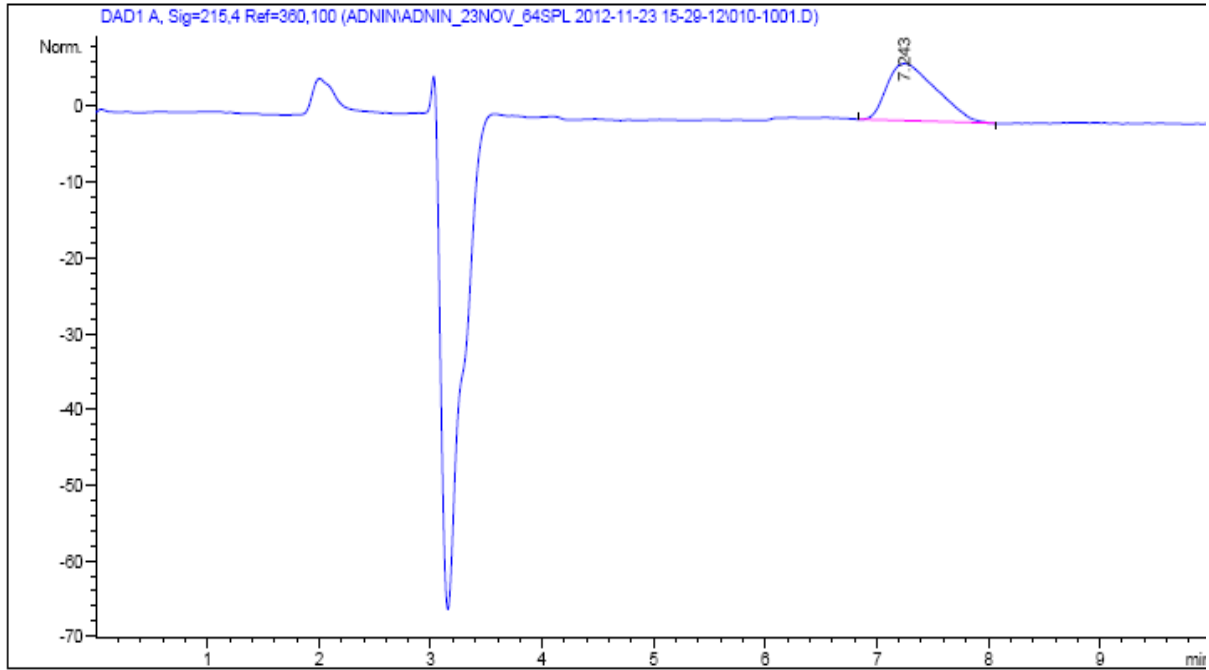


Comment:

Sample Name: ADNIN 0 MIN (I)

```
=====
Acq. Operator   : Jailani                      Seq. Line : 10
Acq. Instrument : Instrument 1                 Location  : Vial 10
Injection Date  : 11/23/2012 5:17:42 PM       Inj       : 1
                                                Inj Volume: 20 µl

Acq. Method     : C:\CHEM32\1\DATA\ADNIN\ADNIN_23NOV_64SPL 2012-11-23 15-29-12\MALAYA_DEA.M
Last changed    : 11/16/2012 8:21:22 AM by Niannah
Analysis Method : C:\CHEM32\1\METHODS\ADNIN_DIPASTD.M
Last changed    : 11/24/2012 11:20:26 AM by Jailani
                (modified after loading)
=====
```



```
=====
External Standard Report
=====
```

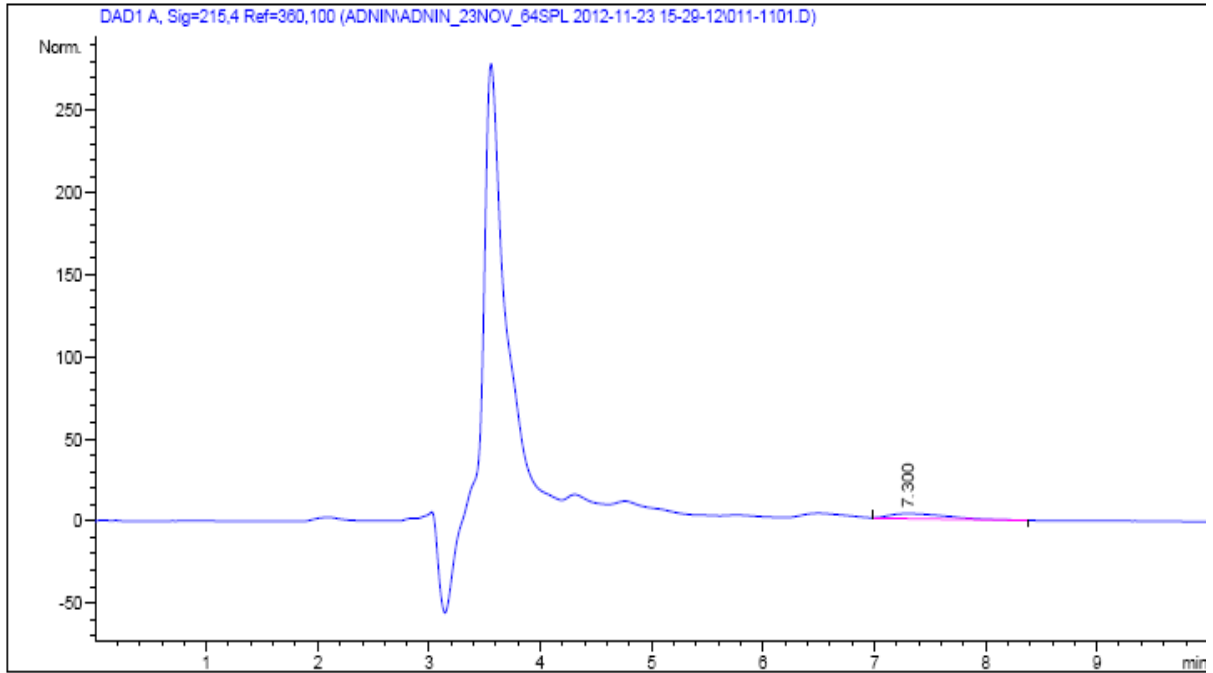
```
Sorted By      :      Signal
Calib. Data Modified :      Monday, November 19, 2012 4:22:59 PM
Multiplier:    :      1.0000
Dilution:      :      1.0000
Use Multiplier & Dilution Factor with ISTDs
```

Signal 1: DAD1 A, Sig=215,4 Ref=360,100

RetTime [min]	Type	Area [mAU*s]	Amt/Area	Amount [g/l]	Grp	Name
7.243	BB +	233.21858	0.00000	0.00000		DIPA

Sample Name: ADNIN 30 MIN (I)

```
=====
Acq. Operator   : Jailani                      Seq. Line : 11
Acq. Instrument : Instrument 1                 Location  : Vial 11
Injection Date  : 11/23/2012 5:29:40 PM      Inj       : 1
                                                Inj Volume: 20 µl
Acq. Method     : C:\CHEM32\1\DATA\ADNIN\ADNIN_23NOV_64SPL 2012-11-23 15-29-12\MALAYA_DEA.M
Last changed    : 11/16/2012 8:21:22 AM by Niamnah
Analysis Method : C:\CHEM32\1\METHODS\ADNIN_DIPASTD.M
Last changed    : 11/24/2012 11:20:26 AM by Jailani
                (modified after loading)
=====
```



```
=====
External Standard Report
=====
```

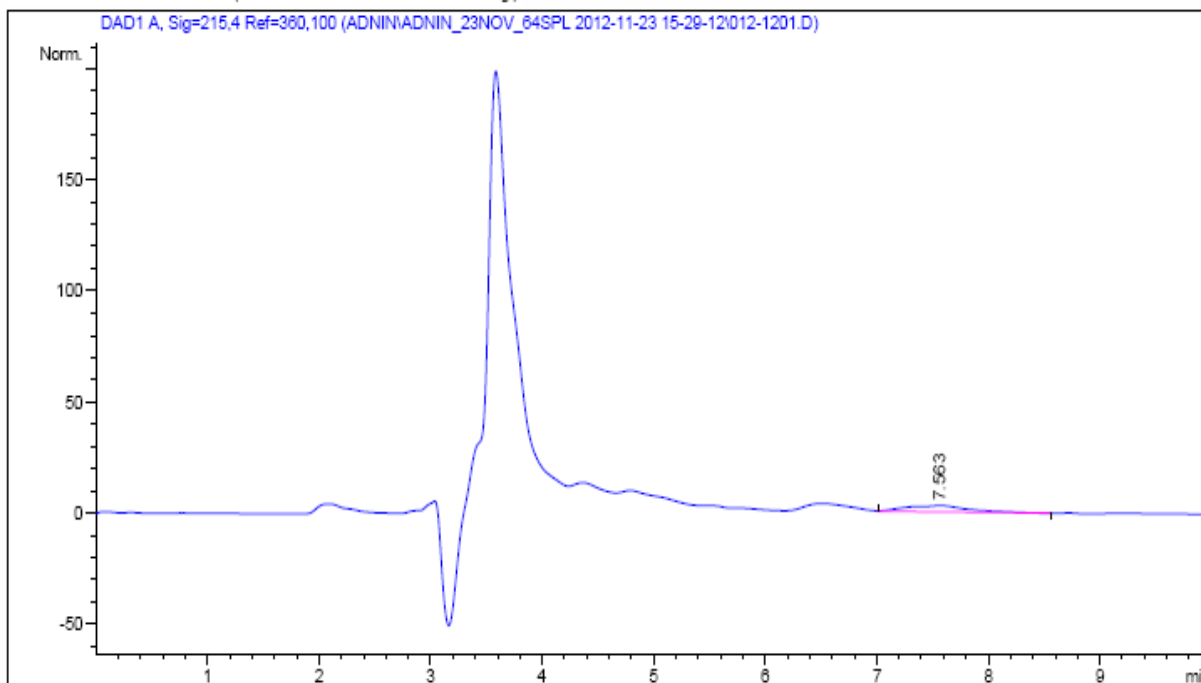
```
Sorted By      : Signal
Calib. Data Modified : Monday, November 19, 2012 4:22:59 PM
Multiplier:    : 1.0000
Dilution:      : 1.0000
Use Multiplier & Dilution Factor with ISTDs
```

Signal 1: DAD1 A, Sig=215,4 Ref=360,100

RetTime [min]	Type	Area [mAU*s]	Amt/Area	Amount [g/l]	Grp	Name
7.300	VB +	121.97828	0.00000	0.00000		DIPA

Sample Name: ADNIN 60 MIN (I)

```
=====
Acq. Operator   : Jailani                      Seq. Line : 12
Acq. Instrument : Instrument 1                 Location  : Vial 12
Injection Date  : 11/23/2012 5:41:38 PM       Inj       : 1
                                                Inj Volume: 20 µl
Acq. Method     : C:\CHEM32\1\DATA\ADNIN\ADNIN_23NOV_64SPL 2012-11-23 15-29-12\MALAYA_DEA.M
Last changed    : 11/16/2012 8:21:22 AM by Niamnah
Analysis Method : C:\CHEM32\1\METHODS\ADNIN_DIPASTD.M
Last changed    : 11/24/2012 11:20:26 AM by Jailani
                (modified after loading)
=====
```



```
=====
External Standard Report
=====
```

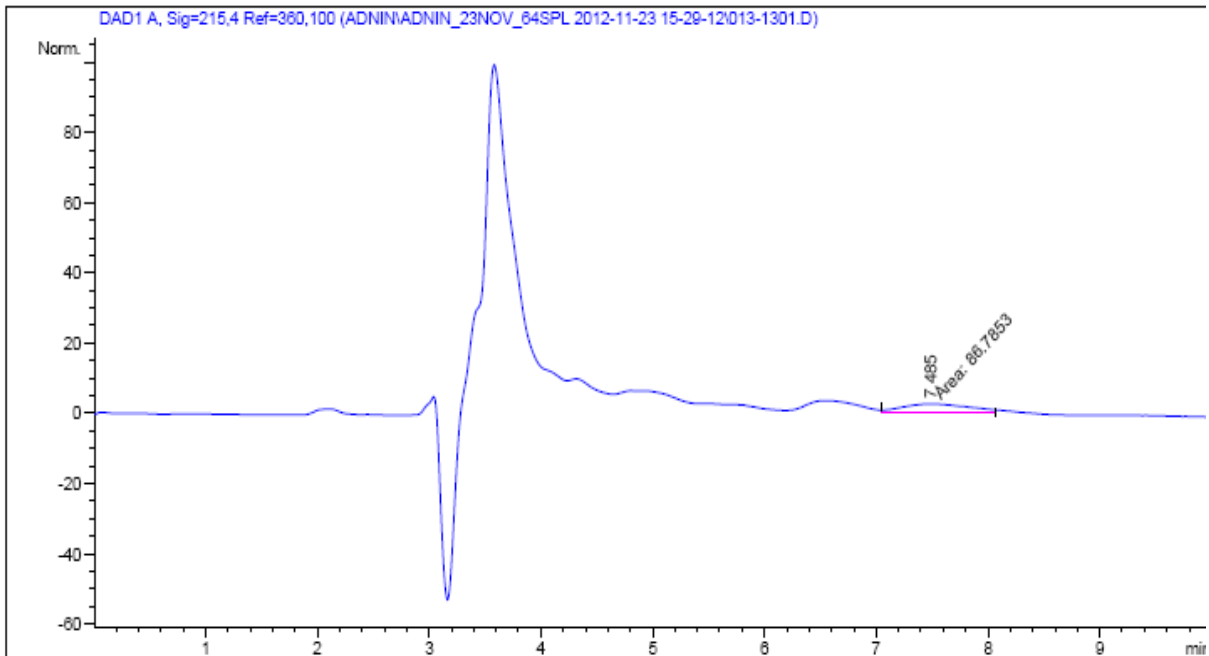
```
Sorted By      :      Signal
Calib. Data Modified :      Monday, November 19, 2012 4:22:59 PM
Multiplier:    :      1.0000
Dilution:     :      1.0000
Use Multiplier & Dilution Factor with ISTDs
```

Signal 1: DAD1 A, Sig=215,4 Ref=360,100

RetTime [min]	Type	Area [mAU*s]	Amt/Area	Amount [g/l]	Grp	Name
7.270	-	-	-	-	-	DIPA

Sample Name: ADNIN 90 MIN (I)

```
=====
Acq. Operator   : Jailani                      Seq. Line : 13
Acq. Instrument : Instrument 1                 Location  : Vial 13
Injection Date  : 11/23/2012 5:53:31 PM      Inj       : 1
                                                Inj Volume: 20 µl
Acq. Method     : C:\CHEM32\1\DATA\ADNIN\ADNIN_23NOV_64SPL 2012-11-23 15-29-12\MALAYA_DEA.M
Last changed    : 11/16/2012 8:21:22 AM by Niamnah
Analysis Method : C:\CHEM32\1\METHODS\ADNIN_DIPASTD.M
Last changed    : 11/24/2012 11:20:26 AM by Jailani
                (modified after loading)
=====
```



```
=====
External Standard Report
=====
```

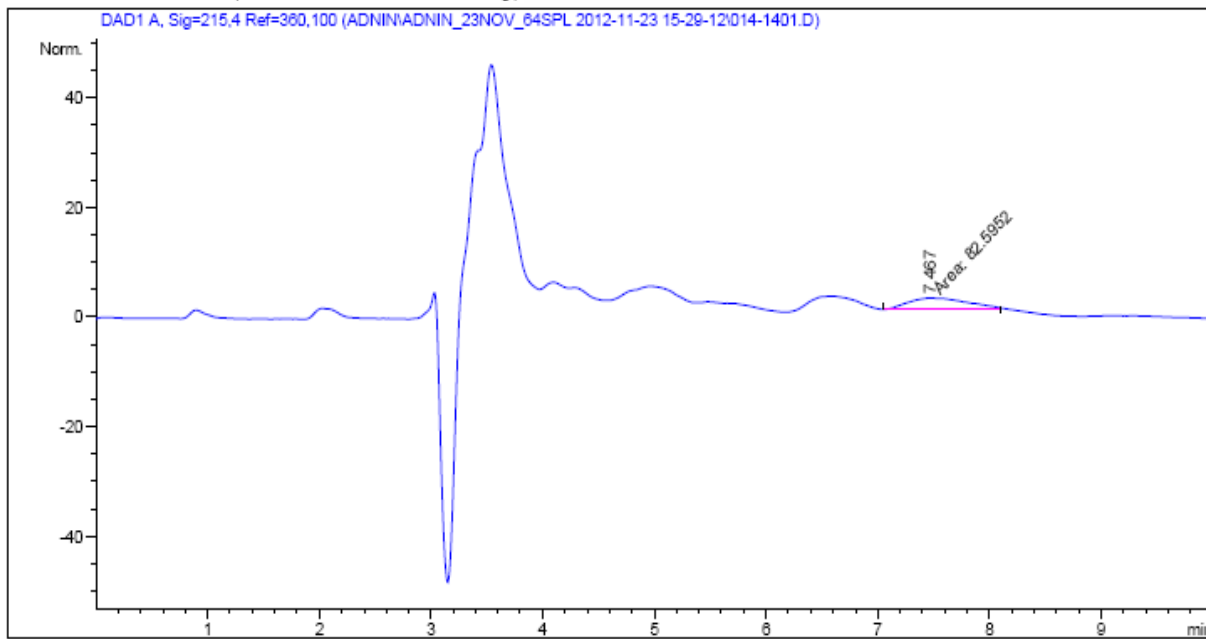
```
Sorted By      : Signal
Calib. Data Modified : Monday, November 19, 2012 4:22:59 PM
Multiplier:    : 1.0000
Dilution:     : 1.0000
Use Multiplier & Dilution Factor with ISTDs
```

Signal 1: DAD1 A, Sig=215,4 Ref=360,100

RetTime [min]	Type	Area [mAU*s]	Amt/Area	Amount [g/l]	Grp	Name
7.270	-	-	-	-	-	DIPA

Sample Name: ADNIN 120 MIN (I)

```
=====
Acq. Operator   : Jailani                      Seq. Line : 14
Acq. Instrument : Instrument 1                 Location  : Vial 14
Injection Date  : 11/23/2012 6:05:22 PM      Inj       : 1
                                                Inj Volume: 20 µl
Acq. Method     : C:\CHEM32\1\DATA\ADNIN\ADNIN_23NOV_64SPL 2012-11-23 15-29-12\MALAYA_DEA.M
Last changed    : 11/16/2012 8:21:22 AM by Niamnah
Analysis Method : C:\CHEM32\1\METHODS\ADNIN_DIPASTD.M
Last changed    : 11/24/2012 11:20:26 AM by Jailani
                (modified after loading)
=====
```



```
=====
External Standard Report
=====
```

```
Sorted By      : Signal
Calib. Data Modified : Monday, November 19, 2012 4:22:59 PM
Multiplier:    : 1.0000
Dilution:      : 1.0000
Use Multiplier & Dilution Factor with ISTDs
```

Signal 1: DAD1 A, Sig=215,4 Ref=360,100

RetTime	Type	Area	Amt/Area	Amount	Grp	Name
[min]		[mAU*s]		[g/l]		
7.270	-	-	-	-	-	DIPA